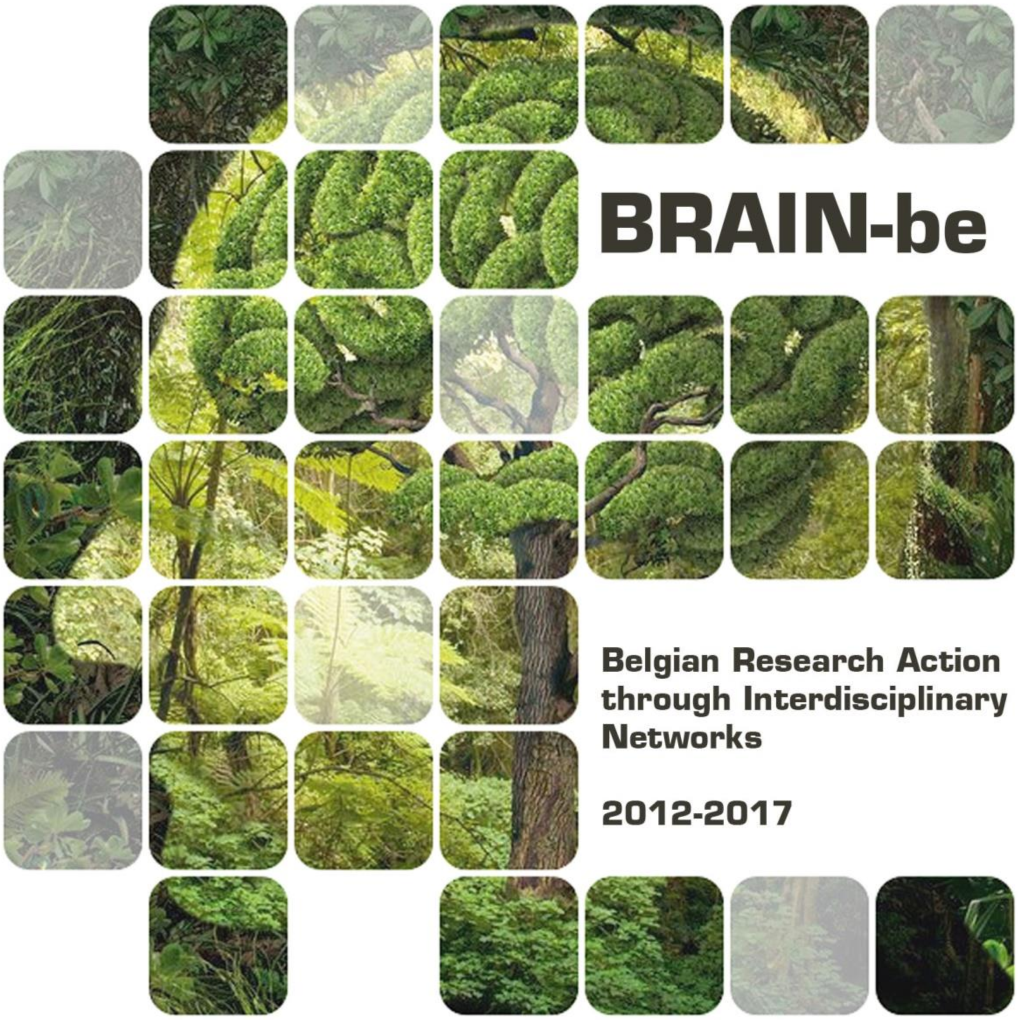


# INDI67

## Developments of Indicators to improve monitoring of MSFD descriptors 6 and 7

Michael Fettweis[1], Erik Toorman[2], Romaric Verney[3], Marion Chapalain[3], Sébastien Legrand[1], Xavier Lurton[4], Giacomo Montereale-Gavazzi[1], Marc Roche[5], Xiaoteng Shen[2], Dries Van den Eynde[1], Vera Van Lancker[1]

[1] Royal Belgian Institute of Natural Sciences, ODNature, Rue Vautier 29, 1000 Brussels, Belgium

[2] Hydraulics Laboratory, Department of Civil Engineering, KU Leuven, Kasteelpark Arenberg 40, 3001 Leuven, Belgium

[3] IFREMER, Laboratoire DHYSED, CS10070, 29280 Plouzané, France

[4] IFREMER, Underwater Acoustics Laboratory, IMN/NSE/AS, CS 10070, 29280 Plouzané, France

[5] Federal Public Service Economies, Continental Shelf Service, Boulevard du Roi Albert II 16, 1000 Brussels, Belgium


NETWORK PROJECT

# INDI67

## Developments of Indicators to improve monitoring of MSFD descriptors 6 and 7

**Contract - BR/143/A2/INDI67**

## FINAL REPORT


**PROMOTORS:** Michael Fettweis (Royal Belgian Institute of Natural Sciences),
Erik Toorman (KULeuven)
Romaric Verney (IFREMER)

**AUTHORS** Michael Fettweis (RBINS)
Erik Toorman (KULeuven)
Romaric Verney (Ifremer)
Marion Chapalain (Ifremer)
Sébastien Legrand (RBINS)
Xavier Lurton (Ifremer)
Giacomo Montereale-Gavazzi (RBINS)
Marc Roche (FPSE)
Xiaoteng Shen (KULeuven)
Dries Van den Eynde (RBINS)
Vera Van Lancker (RBINS)

Published in 2020 by the Belgian Science Policy Office
WTCIII
Simon Bolivarlaan 30 Boulevard Simon Bolivar
B-1000 Brussels
Belgium
Tel: +32 (0)2 238 34 11
http://www.belspo.be
http://www.belspo.be/brain-be

Contact person: Koen Lefever
Tel: +32 (0)2 238 35 51



Fettweis M., Toorman E., Verney R., Chapalain M., Legrand S., Lurton X., Montereale-Gavazzi G., Roche M., Shen X., Van den Eynde D., Van Lancker V. ***Developments of Indicators to improve monitoring of MSFD descriptors 6 and 7***. Final Report. Brussels : Belgian Science Policy Office 2020 – 54 p. (BRAIN-be - (Belgian Research Action through Interdisciplinary Networks))

**TABLE OF CONTENTS**

**ABSTRACT**

## Context

To protect the marine environment more effectively, the European Union adopted the Marine Strategy Framework Directive (MSFD) in 2008, aiming to achieve the Good Environmental Status (GES) of the EU's marine waters by 2020 and to protect the resource base upon which marine-related economic and social activities depend. A major challenge in the implementation of the MSFD is to achieve the necessary scientific knowledge on the marine environment, its processes and the methods to monitor them. The focus of INDI67 is on the evaluation and development of indicators to monitor GES of descriptor 6 and 7. Seafloor integrity (descriptor 6) refers to the structure and functions of the benthic ecosystems. It relates to the comprises physical, chemical and biological properties as well as to spatial and temporal connectedness, avoiding artificial fragmentation of habitats or temporal sealing due to ephemeral sediment deposits or armouring. Hydrographic conditions (descriptor 7) imply that the nature and scale of any long-term changes to the prevailing hydrographical conditions resulting from anthropogenic activities (individual and cumulative), do not lead to significant negative impacts on the benthic and pelagic habitats, functioning or on hydro-geomorphological impacts on the seabed.

## Objectives

The overall objective of INDI67 is to develop and evaluate tools and methods to support the monitoring of MSFD descriptors 6 and 7. The subject is the monitoring of seafloor integrity and hydrography using both modelling and measurements of hydro- and sediment dynamic processes and seabed characteristics. Three parameters have been selected as key indicator, i.e. turbidity, bottom shear stress and seabed/habitat type. These parameters are all related to sea floor dynamics and are strongly linked as changes in seafloor integrity and turbidity occur as a result of the combined force that waves and currents exert on the sea floor. Furthermore, they are witnesses of changes induced by human activities (dredging/disposal, aggregate extraction, constructions, fishery). Turbidity (used both in terms of suspended particulate matter(SPM) concentration and light availability) and bottom shear stress are currently measured and modelled. Bottom shear stress and seabed/habitat type are included in the Belgian MSFD monitoring programme, while turbidity is not yet included as GES indicator.

## Conclusions

The major conclusion with respect to the measuring and modelling of the key indicators turbidity/SPMC, bottom shear stress and seabed/habitat type are:

1) Despite calibration to a reference solution and the use of ISO-normed optical turbidity sensors, model calibration may vary considerably in recorded turbidity for a same SPMC solution across different instruments resulting in instrument-specific turbidity-SPMC relation. Turbidity (or dB for acoustic sensors) should therefore not be used as it is not standardized and will diminish the comparability of the data. Instead, the optical and acoustic sensor output should be transformed into a mass concentration, a unit that is comparable in time and between regions. Monitoring in situ SPMC should follow common guidance and protocols to restrict their measurement uncertainties. The main challenge is now to evaluate model results uncertainty and improve the formulation of natural processes, such as flocculation and bottom shear stress, together with the effects of pressures in the models.

2) The traditional methods to compute the bed shear stress from vertical profiles of velocity, Reynolds stress or turbulent kinetic energy (TKE), which implicitly assume steady conditions, may be incorrect. One of the main problems is that these methods as well as the classical modelling of the bottom shear stress still lacks a physical basis. Nevertheless, given the relatively good correlation between classically modelled bed shear stress and the measured one using the turbulent kinetic energy method and as long as no physical based methods are available for large scale modelling, the use of bed shear stress calculated by classical hydrodynamic models as an indicator for MSFD is appropriate.

3) Some inherent limitations exist when using multibeam technology for the monitoring of seabed/habitat type. They include the complex sediment-acoustic relationships resulting in non-uniform acoustic response per main seabed/habitat type, the uncertainty of the measurements only allows detection of changes of a higher order of magnitude, the variation in time of the state of the transducer. Still, following the procedures developed during the project, the indicator on seabed/habitat type can be mapped and monitored with a reasonable degree of certainty and allow detection of changes and trends meaningful for environmental assessments.

**Keywords**

MSFD, Turbidity, Suspended Particulate Matter, Flocculation, Bed shear stress, Seabed/Habitat type, Acoustic seabed classification, Uncertainty

# 1. INTRODUCTION

There are plenty examples of human activities in coastal environments that affect the physical dynamics or conditions of the water column, the benthic boundary layer and the seafloor. These activities arise from trawling, dredging and dumping, seabed mining and infrastructure works, from the presence of man-made structures in coastal environments or from eutrophication (e.g. van der Veer et al. 1985; Thush & Dayton 2002; Orpin et al. 2004; Fettweis et al. 2009; Stockmann et al. 2009; OSPAR 2010; Baeye & Fettweis 2015; Eigaard et al. 2016; Mengual et al. 2016; van de Velde et al. 2018; Willsteed et al. 2017; Desmit et al. 2018; Madricardo et al. 2019; Mengual et al. 2019). The multitude, geographical spreading and the long-time spans of these activities result in cumulative impacts that are superimposed on the natural variability occurring in these environments. Identifying changes that are not natural requires measuring or modelling the status and trends in the complex and highly dynamic ecosystems of coastal environments. As monitoring all aspects of an ecosystem is impossible due to the range of variables and driving processes, indicators are used that characterize ecosystems and that are cost effective, reliable, easy to monitor or to model and that predict changes that can be averted by ecosystem-based management (Dale & Beyeler 2001; Crowder & Norse 2008; Heink & Kowarik 2010; Burgass et al. 2017).

It is only recently that environmental policies, such as the Marine Strategy Framework Directive (EC-MSFD 2008), have been developed that focus on a holistic approach to marine resource management (Buhl-Mortensen et al. 2017). The Directive is based on an ecosystem approach to manage the impact of human activities on the marine environment through the establishment of targets and associated indicators. Within these legislations each Member State proposes multiple and compound indicators, as well as appropriate monitoring programmes (e.g. Zampoukas et al. 2013). These are listed under the EEAs Central Data Repository (http://cdr.eionet.europa.eu), though effective cross-country evaluation is still hampered by lack and incomplete information.

For the MSFD descriptors 6 (seafloor integrity) and 7 (hydrographical conditions), there are yet no well-established monitoring programmes of physical indicators that allow assessing human-induced changes in the nature and dynamics of physical parameters of the water column and seabed. Some countries have listed turbidity, bottom shear stress and seabed/habitat type (amongst which Belgium and France), though, at best, the programmes are under development and require further investigations. The advantage of the use of physical-based indicators is their relative high efficiency for monitoring and modelling, and their potential to provide an early warning of ecosystem change, preventing adverse effects to biodiversity.

## 2. STATE OF THE ART AND OBJECTIVES

The pelagic zone consists of the water column and the floating living and non-living particles and organisms as well as dissolved matters. Hydrodynamic processes, such as tides, waves, winds and fresh water inputs from land makes it a highly dynamic environment in coastal zones. Nutrient and sediment input from rivers and from resuspension of the seafloor alter the composition and the dynamics of the mineral, biological and biophysical particles in it. On the other hand, the benthic zone is the surface layer of the seafloor with a various composition and typical habitats. The benthic zone receives organic matter from the pelagic zone, decomposes it through remineralization and returns nutrients back to them. The interface between the pelagic and the benthic zone is the benthic boundary layer, a zone where the hydrodynamic forces, the deposition or resuspension of material and the dissipation of hydrodynamic energy through friction occurs. We have selected three indicators that characterize to a part of these three zones: Suspended particulate matter concentration for the pelagic zone, seabed/habitat type for the benthic zone and bed shear stress as the interactive force between both zones. Together their monitoring should allow assessing human-induced physical disturbance (i.e., abrasion, smothering, silting up) and loss (e.g., by fixed structures in the sea), primary criteria underpinning the descriptors 6 and 7, on seafloor integrity and hydrographic conditions, respectively.

### 2.1. The pelagic zone

Water clarity or turbidity is an important parameter to understand marine ecosystems and is mainly controlled by suspended particulate matter (SPM). SPM controls through its influence on the light availability the primary production, and through the concentration and settling of particles in the water column the benthic and pelagic habitats, biodiversity, sediment transport and the fate of pollutants that are attached to the particles. The inherent properties of SPM (i.e. the concentration, size and composition) may change over time depending on the seafloor composition (cohesive and non-cohesive sediments), the hydrodynamics, the measuring height above the bed and biological activity. Sand grains are generally limited to the near-bed layer (bed-load), while fine grained sediments can be found throughout the water column. Charged particles such as clays and polymers may become attached to each other to form fragile structures known as flocs. The composition, size, density, structural complexity, and settling velocity of flocs vary as a function of turbulence, chemical environment (salinity) and bio-chemical composition (e.g. Eisma 1986; Dyer & Manning 1999; Droppo et al. 2005; Fettweis & Lee 2017; Chapalain et al. 2019).

Understanding the dynamical behaviour and the biogeochemical functions of SPM is important as it plays a major role in the in the functioning of the pelagic and benthic ecosystems from the coastal zone to the outer continental shelf (Maerz et al. 2016). The range of SPM concentration found in an area contributes to the depth of the euphotic layer (Capuzzo et al. 2015) and to the diversity and functioning of benthic communities (Van Hoey et al. 2005). SPM consists of inorganic and organic particles, that interact with the environment through physical, biological, and chemical flocculation (e.g. Droppo 2001; Manning et al. 2006; Jago et al. 2007; Verney et al. 2009; Tan et al. 2012). The component microparticles, often covered by biofilm, collide and combine with each other, and as a consequence are aggregated into clusters having larger size, lower density and higher settling velocities than their individual constituents (Shen et al. 2018b). Flocculation kinetics can modulate sediment bed exchanges and determine concentration dynamics (Letter & Mehta 2011). Recent publications have underlined the importance of bio-medicated flocculation and its impacts on SPM dynamics and have shown that biological effects are of comparable importance with other physical (e.g., turbulent shear and SPM concentration) and chemical (e.g., salinity, PH and ionic strength) parameters (Mietta et al. 2009; Tang & Maggi 2016; Shen et al. 2018b; 2019b).

## 2.2. The benthic zone

The benthic zone stretches across the lowest level of the body of water that defines the Ocean: the seabed. A broad variety of habitats exists both inside (i.e. infaunal communities) and above the seabed (i.e. epifaunal and demersal communities), depending on an intricate combination of environmental factors including substrate type (i.e., mud, sand, gravel), depth, hydrodynamics and other local environmental conditions. Benthic life (e.g., shellfish, flatfish, worms, bacteria) is strongly bound to these natural characteristics and dynamics, as well as the quality of the seabed. Abiotic proxies such as gravel, providing structural complexity, and/or sand, providing suitable habitat for infaunal species, are key proxies to be considered when studying and characterising the seafloor. The production of abiotic maps, as those originated form multibeam echosounder (MBES) acoustics in the framework of this project, assume that the distribution of benthic life follows environmental gradients such as those of substrate type (McArthur et al. 2010) and exploits the geophysical data to predict accurately and over continuous spatial scales otherwise hardly accessible parameters and material properties of the seabed. A healthy structure and functioning of marine ecosystems depend on the physical, chemical and biological characteristics of the seafloor, including natural spatial connectivity or seafloor integrity (Rice et al. 2012).

## 2.3. The interface between the benthic and pelagic zone

The conceptual relationship between floc diameter, SPM concentration and shear stress proposed by Dyer (1989) and later extended to include biological effects (Lai et al. 2018; Shen et al. 2018b, 2019b) shows that turbulent flow predominantly controls particle aggregation and the settling velocity of the flocs. The large flocs that occur during slack water will quickly settle, increase the near-bed SPM concentration, and form lutoclines that separates the water column with generally lower SPM concentration from the fluffy surface bed layers (Mehta 1986; Winterwerp 2002; Becker et al. 2013). The particle-turbulence interactions and the stratification-induced turbulence damping contribute to the formation and stability of the lutocline and thus of these High Concentration Mud Suspensions (HCMS) or fluid mud layers (Le Hir et al. 2000; Toorman 2002; Winterwerp 2006).

## 2.4. Aim of the project

The aim of the project is to evaluate the indicators on SPM, bottom shear stress and seabed habitat type in relation to descriptors 6 and 7. More specifically the uncertainties associated with the measurements and the modelling aspects need addressing, as well as the processes that need to be included in models in order to increase the precision of numerical simulations.

## 3. METHODOLOGY

For all three proposed indicators a number of scientific and operational challenges are addressed related to the understanding of processes (flocculation, turbidity and SPM dynamics, seabed dynamics), the development of new process-based modules in existing numerical models (flocculation, drag modulation, current-wave bottom shear stress, seabed composition), and the assessment of the uncertainty of measurements and models.

### 3.1. SPM concentration, turbidity and floc size

#### 3.1.1. In situ measurements of turbidity and SPM concentration

Turbidity refers to the optical water cloudiness caused by suspended particles and dissolved substances, which scatter and absorb light (Downing 2005; Ziegler 2003; Gray & Gartner 2009). Turbidity does not have a SI unit, is not uniquely defined and depends strongly on the applied protocols. It is thus an arbitrary unit that is incomparable to measurements taken at other times and places or with different turbidity meters, which diminishes the comparability of turbidity data for scientific purposes (Downing 2006). There are two international recognized methodologies for determining turbidity: the ISO Method 7027 (ISO 1999) and the American EPA Method 180.1 (EPA 1993). Both estimate turbidity, for the ISO method it is in formazine Nephelometric Units (FNU), and for the EPA method in Nephelometric Turbidity Units (NTU), respectively, and in both methods, the optical sensor to be used is a nephelometer that must measure side-scattered light at 90°. There are, however, some differences between the two methodologies. Turbidity following the EPA method is poorly defined. The strengths of the ISO method include the use of a stable monochromatic near infrared light source of 860 nm with low absorbance interference with samples, which is critical in reducing the impact of particulate and coloured dissolved organic matter absorption and in having low amounts of stray light (Sadar 1999). Sensors designed according to the ISO definition of turbidity provide thus a better basis for the comparability of measurements than those designed following the EPA specification (Barter & Deas 2003, Nechad et al. 2009; Bright et al. 2018).

SPM is a mixture of clay to sand-sized particles that can be detected in suspension and that consists of varying amounts of minerals from physico-chemical and biogenic origin, living and non-living organic matter, and particles from human origin. The particles are considered to be in suspension as long as they do not form an interconnected matrix of bonds that prevents their mobility; this is the case when the concentration is below the gelling point (McAnally et al. 2007). The inherent properties of SPM (i.e. the concentration, size and composition) may change over time depending on the seafloor composition (cohesive and non-cohesive sediments), the hydrodynamics, the measuring height above the bed and biological activity. Sand grains are generally limited to the near-bed layer (bed-load), while fine-grained sediments can be found throughout the water column. Long-term and high frequency data series of SPM concentrations (SPMC) are typically collected indirectly with autonomous sensors that measure either the optical beam attenuation as a percentage of light transmission (Moody et al. 1987; Spinrad et al. 1989; Agrawal & Pottsmith 2000), the back- or sidescatter intensity of light in volt or factory calibrated turbidity units, or the acoustic backscatter in counts or volts (Thorne & Hanes 2002; Downing 2006; Rai & Kumar 2015). In addition to these sensors gravimetric measurements of filtered water samples are generally used as ground truth reference (e.g. Neukermans et al. 2012; Röttgers et al. 2014; Fettweis et al. 2019). The combination of indirect and reference measurements requires two main calibration steps (sensor and model parameter calibration) at different moments during the workflow to extract reliable and homogeneous SPMC. These calibration steps are essential for relating changes in calibration constants (both sensor and model parameter constants) to either sensor degradation or to natural variability in SPM inherent properties. Changes in SPM properties and concentration might be related to seasonal and geographical variations. The latter is typically occurring along the gradients from the estuary, coastal zone towards the offshore (Fettweis et al. 2006; Becker et al. 2013; Maerz et al. 2016; Many et al. 2016; Druine et al. 2018). We have made a detailed analysis of the uncertainty associated with measurements of SPMC in order to increase the applicability of an indicator based on SPMC (Chapalain et al. 2019; Fettweis et al. 2019).

The relationship between the signal from an optical backscatter sensors (OBS) or sidescatter sensors (nephelometer) and the SPMC is almost linear as long as the sensor is not deployed in highly concentrated waters (Downing 2006), and the simplest model is a linear regression model. The same holds for single point acoustical sensors (ADV) or for the first bin of a profiling acoustical sensor, where the target volume is very close to the sensors. As far as SPMC are lower than several g/l, a direct empirical relationship can be built such as $log_{10}(SPMC)\sim S_v$, where the acoustic volume backscatter strength $S_v$ can be related to the signal/noise ratio (Fugate & Friedrichs 2002; Voulgaris & Meyer 2004; Verney et al. 2007; Ha et al. 2009; Salehi & Strom 2011).

For profiling acoustic sensors, the sonar equation should be considered to correct for the signal loss along the acoustic path. The conversion factor from counts to dB, as commonly used in acoustics, is typically provided by the manufacturer. Close to the transducer, the acoustic signal has to be corrected for near-field effects (Downing et al. 1994) and for ringing effects that may affect the first bins, in particular when blank distance is set too small in the configuration parameters. Corresponding data cannot be corrected and should be discarded (Muste et al. 2006). A formulation for the water absorption coefficient was proposed by e.g. Francois & Garrison (1982a, b) and later simplified by Ainslie & McColm (1998), who showed that their result did not differ from the original equation more than the accuracy error. The sonar equation yields the so-called water-corrected backscatter, which is a property of the suspension at all locations along the acoustic path. Subsequent processing depends on the SPMC. In case of moderately turbid environment, i.e. lower than O(100) mg/l and depending on the acoustic frequency, sound attenuation by SPM is usually neglected as it is one or two orders of magnitude lower than the water absorption coefficient (Ha et al. 2011). SPMC is then either determined by applying an appropriate calibration, similar to single point optical sensors, or by a theoretical acoustic model. In the latter case, physical properties of the transducer and of the SPM must be exactly known, which are rarely available. If SPMC exceeds several 100 mg/l, sediment absorption should be considered. However, this term is a function of the SPMC, which is also the unknown of the calculation. The inversion problem is solved by iterative methods (Thorne et al. 1994; Holdaway et al. 1999). This technique is efficient but requires assumption or knowledge about transducer physical properties, SPM characteristics (size, density) and is based on the choice of an acoustic model adapted to the observed SPM, and may in some specific case exponentially propagate uncertainties and fail to estimate SPMC (Becker et al. 2013). Theoretical acoustic models were originally built to simulate the physical interactions between particles and the acoustic signal (Sheng & Hay 1988, Medwin & Clay 1998) and were applied to sand particles in suspensions (Thorne & Hanes 2002). These models were later adapted to represent low density aggregates of SPM (Stanton 1989; MacDonald et al. 2013; Thorne et al. 2014) and were shown to correctly estimate SPMC in estuarine environments (Sahin et al., 2017). Differences between models mainly appear in the methodology to calculate the total scattering and backscattering cross section as well as the compressibility of flocs and their ability to interact with sound. Merckelbach & Ridderinkhof (2006) and Nauw et al. (2014) observed that at strong currents (>1 m/s) acoustical backscatter exceeds the linear relationship to sample SPMC noted at lower currents. This was not due to changes in the particle-sizes and the non-linearity was compensated for, based on a model that suggests a transition from random phase to coherent particle backscatter by turbulence-induced variability in in the spatial distribution of SPMC (Merckelbach 2006). More research is however required to understand the cause of this effect.

As mentioned above, calibration models are sensor-specific and strongly related to the characteristics of SPM (composition, size, shape, density…) that can vary with hydrodynamic forcing's (e.g. calm weather versus storms) and seasonally. Additional issues and sources of uncertainties are identified (Fettweis et al. 2019): battery depletion and power supply-related drifts; biofouling on optical windows, acoustic transducers and in the neighbouring environment; air and gas bubbles; water sampling strategy and human errors. Most of these issues cannot be corrected and measurements must hence be discarded from analysis and datasets.

### 3.1.2. In situ measurements of SPM particle size

Complementary to SPMC measurements, particle size measurements are essential to evaluate the floc size dynamics and the SPM settling fluxes. In coastal systems, particle size distribution measurements are conducted from laser-based or camera-based systems. The latter is based on prototypes, while the former is the mostly used, with commercially available systems (e.g. LISST instruments), and then will be used in this study. The LISST 100 instrument has become a standard measuring instrument for particle size spectra and volume concentrations (e.g. Agrawal & Pottsmith 2000). LISST measurements consist in emitting a laser beam which is scattered by particles at small forward angles and detected by ring detectors. The particle size distribution (PSD) is then back-calculated using an optical model. Two models are available. The first one is based on the Mie theory assuming that particles have a spherical shape while the second one is based on random shaped particles (Agrawal et al. 2008). The volume concentration is estimated using the particle size distribution together with an empirical volume calibration constant that is specific to spherical or random shaped particles. Uncertainties using LISST 100C detectors may arise to non-spherical flocs (such as complex aggregates), to floc sizes exceeding the instrument range, to a too high or too low SPM concentration or to stratification of the water column (Chapalain et al. 2019; Chapalain 2019).

The effect of the floc shape on LISST measurements is complex to estimate, and can only be evaluated through the choice of the inversion model, i.e. spherical or random shape, in the LISST post-processing. The main consequence of the model choice for a given distribution is a shift towards smaller class sizes, without changing significantly the spectrum shape. The LISST provides reliable measurements along an operational concentration or turbidity range. In low SPMC environments (i.e. transmission above 90% or SPMC below 5 mg/l), LISST measurements are strongly dependent on the background quality, and instabilities in raw signal measurements can produce artefacts and bad detection particles, mainly in the largest size classes. It is then recommended to record time-average measurements for improving data reliability. In high concentration ranges, multiple scattering occurs and can generate additional unrealistic signal in the extreme size classes. It is then recommended to discard data with transmission measurements below 20%-30%. This upper limit corresponds to SPMC values of several 100 mg/l, i.e. far lower than the saturation level. The last source of uncertainty regarding LISST measurement is certainly the most critical in coastal waters, as related to density stratification. This effect known as the Schlieren Effect (Styles 2006) is caused by the deviation of the laser beam due to salinity gradients and related changes in refraction indices. This effect increases the signal recorded by the inner detectors and artificially increases the volume concentration in the largest size classes. The buoyancy frequency is an efficient metrics to qualify the LISST data (Mikkelsen et al. 2008), with a threshold value depending on the SPMC level: the larger the SPMC, the lower the buoyancy frequency threshold (e.g. 0.8 $s^{-1}$ in for SPMC values O(100 mg/l) and 0.025 $s^{-1}$ for SPMC values below 10mg/l).

Within the operational limits, the LISST100 is useful for evaluating particle size dynamic and, combined with SPMC data, for estimating floc density, floc structure (fractal dimension) and floc settling velocities (Fettweis & Baeye 2015; Fettweis & Lee 2017; Chapalain et al. 2019). In the mouth of the Seine estuary, at the interface between the estuary and the coastal sea, it was observed the dominant influence of the turbulence on floc formation/breakup at the tidal scale, and an increase in the flocculation intensity and floc strength with the chlorophyll-a content (Chapalain et al. 2019). The consequences of the influence of the organic matter content on floc settling velocity show a cross-shore and seasonal pattern. Close to the coast, the presence of mineral SPM together with a favoured flocculation lead to slightly higher settling velocities while offshore, where organic matter dominates SPM, organic-rich flocs are characterized by lower settling velocities (Fettweis & Lee 2017). Seasonality is characterized by a higher SPM concentration in the benthic boundary layer during summer, but lower in the remaining water column. During winter, the opposite is found. The floc size and settling velocity have an opposite seasonality: smaller flocs and thus settling velocities occur in winter and larger flocs and settling velocities in summer (Fettweis & Baeye 2015). The next step will consist in confronting in situ observation and 3D numerical models simulating explicitly flocculation dynamics. The measurements have shown that the near-bed processes do influence the SPM transport on different time scales and that significant part of the SPM fluxes occur in the benthic boundary layer. Models show promising results when the bed shear stress closure incorporates additional dissipation mechanisms (i.e., interparticle friction and collisions, and particle wake turbulence) that are important in the high SPM concentration layers occurring near the bed (Bi & Toorman 2015).

### 3.1.2. Modelling flocculation

One target of the project is to develop and/or evaluate the use of environmental indicators such as bottom shear stress, turbidity and seabed habitat, which strongly relate to the transport of suspended particles in the water column, for a risk assessment of ecosystems. However, up till now the predictions of the behaviour of SPM are still unsatisfied and sometimes are difficult to match observations. One important reason is due to the limited understanding of the flocculation processes of mineral-biological particles and their implementation in numerical models. Therefore, previously developed flocculation models (e.g. Lee et al. 2011) have been improved, simple methods to include biofilm growth have been proposed, and the flocculation model has been implemented to the Belgian coastal area with open TELEMAC (Shen et al. 2018a, 2018b, 2019a, 2019b).

The two-class population balance equation (2CPBE) flocculation model developed by Lee et al. (2011) has been improved to include three classes of particles (3CPBE), in order to describe the representative sizes and mass fractions of microflocs (≤ 30 µm), macroflocs (30 − 200 µm) and megaflocs (≥ 200 µm) (Shen et al., 2018a). Five tracers were focused on: (1) $N_P$ – number density of microflocs only in suspension, (2) $N_{F1}$ – number density of macroflocs in suspension, (3) $N_{T1}$ – number of microflocs in macroflocs, (4) $N_{F2}$ – number density of megaflocs in suspension, and (5) $N_{T2}$ – number of microflocs in megaflocs. With a fixed size of microflocs, the sizes of macroflocs and megaflocs can be found from the value of the tracers. In case the size of third class was fixed, $N_{F2}$ is omitted and it becomes four tracers. With this framework, the 3CPBE can be implemented in the open TELEMAC, with their source and sink terms programmed in the subroutine source_trac.f. This improvement results in a better representative of large megaflocs which can be easily observed typically formed after the peak algae bloom period. Moreover, it makes it possible to include a process-based flocculation model to better predict the dynamic settling velocities and deposition rates in 3-D large-scale coastal and ocean models. Besides validations with settling column experimental results, field data in the MOW1 station was used to validate our model (Shen et al. 2018a, 2018b)

It is still an open question about how to interpret a floc size distribution (FSD). Are three classes good enough? If so, how can we address the standard deviations of subordinate FSDs? If not, how can the entire FSD curve efficiently been mimicked? Keeping these questions in mind, we have applied the extended quadrature method of moments (QMOM) assuming that the final FSD is composed of a set of lognormal distributions with a common standard deviation, to better display the FSDs, compared with previous methods which represent FSDs with a series of delta functions (Shen et al., 2019a). The common standard deviation was determined empirically as a function of mean size of the FSD. With this simplification and selecting the number of subordinate FSDs as $N = 2$, only four tracers were used to mimic the entire FSD for their representative sizes and weights of microflocs and macroflocs. Although further increasing $N$ sometimes may cause numerical instabilities, the future of using this approach to represent FSDs and efficiently coupled with large scale models is still promising if with necessary modifications. In reality, QMOM-based PBE (QMOM-PBE) and multi-class based PBE (MCPBE) have their own pros and cons. For example, QMOM-PBE could set a continuous initial distribution of microflocs but MCPBE can only use one representative size $l_p$; QMOM-PBE could test relatively complicated fragmentation distribution functions (such as lognormal, binominal and parabolic fragmentations) which is difficult for MCPBE to work with; QMOM-PBE is easy to control for different number of size classes (by only changing the parameter $N$) while MCPBE have to re-program the source and sink terms of the tracers; MCPBE have to give seeded particles which may influence the simulated FSDs while QMOM-PBE does not have to. However, current tests show that MCPBE are more robust than high-order QMOM-PBE since the latter involves a process to extract the FSDs from their moments which is a numerically ill-conditioned issue, and MCPBE is also more efficient than QMOM-PBE.

The feedbacks and interactions between the successions of various biologically, biogeochemically and sedimentologically interactive systems have recently gained much interest in the scientific community (e.g. Regnier et al. 2013; Fettweis et al. 2014; Maerz et al. 2016; Lee et al. 2019; Schartau et al. 2019). By changing the cohesive properties, biological processes change the stickiness of mineral particles to the extent that inherent properties of primary particles (clays) can become of secondary importance for sedimentation-erosion processes and bedform development (Malarkey et al. 2015; Maerz et al. 2016). Specifically, the mechanisms behind these bio-physical interactions and the ecosystem scale consequences of them are not well known. We contributed to the bio-physical interaction in SPM dynamics by proposing a simplified biofilm growth model that highlights the biological effects on cohesive sediment flocculation (Shen et al. 2019b). In natural environments, biodegradation of organic matters releases sticky organic biopolymers such as the extracellular polymeric substances (EPS). Biofilms may attach to the mineral particles and thus change the size and density of bio-mineral flocs. Previous studies either ignore the biological processes or include a large number of water quality parameters which does not help to improve the model predictions. In the biofilm growth model, the net increase of aggregate size due to biofilm effects is assumed to follow the logistic growth pattern, which is controlled by two parameters: the specific growth rate $\eta$ and the carrying capacity $K$. The Monod equation is used to determine $\eta$ by assuming that the biofilm growth is nutrient dependent. Dissolved organic carbon and light may be the other factors influencing biofilm growth for other circumstances. The carrying capacity $K$ describes the maximum floc size under a specific environment which is assumed to be proportional to the Kolmogorov length scale and thus the turbulent shear rate. Again, settling column experiments with an averaged shear rate and field data at MOW1 station at Zeebrugge were used to validate the model. It shows an increase in settling velocity due to biofilm coating. This provided a simple way to illustrate biological flocculation rather than using tedious microbe functions. Linking with water quality library in the future (such as AED2, see http://aed.see.uwa.edu.au/research/models/AED/), the parameters $\eta$ and $K$ can be better investigated to find the FSDs of SPMs. At that time, the harmful pollutants attached to the aggregates can be further studied as a warning for ecosystem changes.

## 3.2. Seabed/Habitat type

The Belgian State (2012) formulated two seafloor integrity-related indicators for which multibeam echo sounding (MBES) was selected as the mapping and monitoring technology. The first one indicates that the areal extent and distribution of the European Nature Information System (EUNIS) level II, as well as of the gravel beds, remain within the margin of uncertainty of the sediment distribution with reference to the Initial Assessment map. The second mentions that the ratio of the hard (gravel) substrate surface area to the soft (sand) substrate surface area must not show a negative trend.

Hereafter, the methodological workflow is described that enhanced the exploitability of MBES backscatter (and bathymetry and its derivatives) in the MSFD monitoring framework. Regarding the acquisition and processing of high-frequency MBES backscatter and bathymetry data, rigorously standardised protocols have been developed that align closely to the recommendations set out by the Backscatter Working Group (BSWG) piloted by the Geological and Biological Habitat Mapping Community (GEOHAB), see http://geohab.org/bswg and Lurton & Lamarche (2015).

### 3.2.1. Multibeam data acquisition and processing

High-frequency (300 kHz) multibeam surveys were conducted over the course of three years (2015-2018) covering nearshore to offshore areas of the BPNS. Kongsberg Maritime systems EM3002 dual and EM2040 installed on RV A962 Belgica and Simon Stevin, respectively. Data were logged using Kongsberg Maritime's acquisition software SIS. Both echosounders were operated in high-density equidistant mode, forming 508 (1.5°x1.5°) and 800 (1°x1°) soundings per ping, respectively for the EM3002 and EM2040 dual systems. Real-time corrections for sound velocity in the water column were obtained by a Valeport mini-SVS sensor installed in proximity of the transducers. Precise positioning and vessel motion were recorded by an MGB Tech with Septentrio AsteRx2eH RTK heading receiver and a Seatex MRU 5 unit for the EM3002D, and by an MGB Tech with Septentrio AsteRx2eL RTK heading receiver and a XBlue Octans motion sensor for the EM2040D. The EM2040 on RV Simon Stevin was upgraded to a dual system during 2017, whereas the EM3002D remained unchanged throughout the time span of acquisition.

### 3.2.2. Multibeam bathymetry and backscatter

Bathymetry data processing was carried out using QPS Qimera© (v1.2.4.429a). Real-time kinematic (RTK) and GPS modelled tide solutions were used to correct the real-time navigation data. In turn, manual edits were applied to the soundings, referenced to the Lowest Astronomical Tide datum. Data were gridded to a 5 m (Montereale Gavazzi 2019) or 1m horizontal resolution (Montereale Gavazzi et al. 2018, 2019). Backscatter data processing was carried out in QPS Fledermaus Geocoder© (FMGT) software. To allow data inter-comparison, a strictly standardised procedure was maintained during the processing phase. FMGT mosaic processing parameters ("pipeline settings") were maintained as close as possible to the default settings of both echosounder models. All beams from the "beam time series" were kept. Absorption in the water column was compensated by the absorption coefficients (sensu Francois & Garrison 1982b, 1982a) in the raw datagram. This coefficient was updated every 30 minutes while logging the data and computed according to the local surface seawater properties. The necessary water-medium parameters were obtained by the On-Board Data Acquisition System (ODAS), logging these data at 10-s intervals. Using FMGT, the angular dependence was compensated leaving parameters as close as possible to the default settings i.e. an Angular Varied Gain window size of 300 pings and the default "mosaic processing" settings. the sole modification was the average reference angle used to normalize the data, set in the range 43°- 47°. The true ensonified area was accounted for by inclusion of a Digital Terrain Model (DTM) in the processing.

### 3.2.3. Ground-truth data acquisition and processing

Ground-truth data were acquired in complement to each MBES survey (i.e. within ~48 hours from the acoustic survey completion) and are therefore closely representative of the seafloor status at the time of the survey. The sampling effort was planned in such a way that it was representative of the area (i.e. backscatter map) being sampled. Several gears were tested and deployed including physical (i.e. grab and core sampling), optical (videography) and sediment profile imaging (SPI). The choice of gear was largely dictated by the expected type of substrate being sampled. For example, the Hamon grab sampler and video observations were the instruments of choice within the gravel areas, whereas box cores, Van Veen grabs and SPI were favoured within the soft sediment areas.

Ground-truth data were described in terms of surficial substrate type. Sample coordinates were geo-referenced and automatically corrected during the acquisition for the DGPS antenna layback accounting for the main source of positional error. Samples were described combining visual and expert observations with grain-size parameters derived by sediment analysis using a Malvern Mastersizer 3000 and processed in GRADISTAT (Blott & Pye 2001). Since only the fraction ≤1 mm could be analysed by the Malvern, the percentage of the coarse fraction (bioclastic detritus and gravel) was visually estimated thus scoring a qualitative gravel percentage. Wherever samples have been used to train and validate a predictive model, the sample collections were split according to a random stratified split rule (70 – 30 for training and validation subsets respectively). Only features visible at the water-sediment interface were described (except for Hamon grab samples where the sampling does not preserve the vertical integrity of the seafloor) and summarised into thematic classes according to two classifications schemes commonly applied in the European underwater mapping context, i.e. the broader EUNIS habitat III classification (e.g. Galparsoro et al. 2012) and the finer Folk (1954) classification , allowing for a more detailed distinction of sediment classes.

### 3.2.4. Seamless merging of disparate datasets

To allow merging of the disparate backscatter datasets and produce a seamless map of reflectivity, a methodology similarly to Hughes-Clarke et al. (2008) and Misiuk et al. (2018) was applied. The approach may be referred to as a “cross calibration propagation” and consists of selecting a reference survey and adjusting all other surveys by overlap to the nominal truth. Here the overlap refers to a highly stable relative calibration reference area, i.e. the Kwintebank swale (Roche et al. 2018). The resulting backscatter map (Fig. 3.4 in Montereale Gavazzi 2019) shows the seamless character achieved after applying the offsets and merging the surveys. The cross-calibration propagation was carried out by applying the dB empirical offsets directly to the mosaicked compensated backscatter grids. Considering the processing chain of FMGT (Lamarche & Lurton 2018; Schimel et al. 2018), it is assumed that all angle dependencies have been compensated for, i.e. those caused by the MBES directivity pattern and those from the backscatter angular dependence. Therefore, the mosaic is representative of the average backscatter strength of the seafloor normalised to a conventional average reference angle in the range 43°-47°, including the systems sensitivity. As such, the dB offsets represent average shifts at 45° and by referring all surveys and sounders to the same nominal truth, the sounder sensitivity is corrected for, leaving only the seamless character of the average response; lawful for a regional compilation of backscatter maps.

### 3.2.5. Acoustic seafloor classification

Different statistical methods have been employed towards the study of sediment-acoustic relationships. Relationships between MBES backscatter and sediment type were initially investigated using boxplots summarising bathymetry and backscatter statistics grouped by EUNIS III and Folk sediment categories. This provides insights into the class separation potential (i.e. the discriminative power of the data in respect to the proposed classifications schemes). Cumulative distributions of backscatter and bathymetry were compared between the entire study area and training and validation sample sets to visually assess their representativeness, thus their viability for the Acoustic Seafloor Classification (ASC) routines. Linear regression was used to assess relationships between the average backscatter extracted from a 25 m buffer around each sample location and the median grain-size diameter (D50). A more insightful analysis was based on relationships between percent weight of individual size fractions and the mean backscatter (Fig. 3.1B in Montereale Gavazzi 2019), where sandy and gravelly areas predominate.

Two modelling approaches, i.e. unsupervised clustering via k-means (Hartigan & Wong 1979) and supervised classification via Random Forest (Breiman 2001), have been tested to predict class membership of both classification schemes over the full extent of the MBES datasets (Montereale Gavazzi et al. 2018; Montereale Gavazzi 2019). K-means clustering is amongst the most widely applied data clustering technique, including numerous examples in the literature (e.g. Hewitt et al. 2004; Fonseca & Calder 2007; Alevizos & Greinert 2018; Snellen et al. 2018; Fezzani & Berger 2018). Supervised Random Forest (RF) was selected to test the performance of backscatter in combination with bathymetry alone, as well as in combination with a set of derivatives of the primary MBES data. RF models have been reported to achieve high predictive accuracy (e.g. Diesing et al. 2014; Diesing & Stephens 2015; Ierodiaconou et al. 2018; Turner et al. 2018; Porskamp et al. 2018) and have generally proven highly successful in remote sensing applications (Belgiu & Drăguţ 2016). A detailed discussion of the clustering methods can be found in Montereale Gavazzi (2019, Ch. 3).

### 3.2.6. MBES derivatives, selection and model tuning

To enhance the local characterisation of the primary MBES dataset and identify homogenous areas of substrate and morphology using the supervised Machine Learning approach, a set of secondary spatial derivatives were produced from backscatter and bathymetric grids (Table 3.2 and Fig. 3.7 in Montereale Gavazzi 2019). Selection of the spatial layers was based on their expected influence on the distribution of sediment type and due to their ability to enhance the predictive accuracy of seafloor substrate and benthic habitat thematic models in previous research (e.g. Lecours et al. 2016; Rattray et al. 2013; Ierodiaconou et al. 2018).

A feature selection procedure was undertaken to identify the subset of relevant variables from the initial input layers. Despite Random Forest being able to handle a large number of highly correlated variables, it has been shown that using only a relevant sub selection of variables improves predictive accuracy as well as computation times (Li et al. 2016). The Random Forest Boruta wrapper function (Kursa & Rudnicki 2010) was used on the reduced data set to assess the relative importance of various subsets of input features over multiple runs of the algorithm and to provide an estimate of predictor importance.

Particular attention has been placed on the accuracy assessments of the models used. Thematic maps do not serve their scope if their information is not directly associated to an objective quantitative measure of accuracy: metrics expressing the “goodness of mapping” allow to identify the presence, quantity, distribution and nature of the misclassification error, enhancing the utility of the map in a decision-making scenario. Therefore, the accuracy assessment phase of any predictive mapping study should address the following points (Stehman & Czaplewski 1998): (1) What is the error frequency or how often does the map not agree with reality?; (2) What is the nature of the errors or which classes are not mapped correctly, and with which other classes are they confused?; (3) What is the magnitude of errors or how serious are they for a decision maker?; (4) What is the source of the errors or why did they occur? As such, the accuracy of the thematic models produced was assessed in terms of global accuracy (A) with corresponding 95% confidence intervals and Kappa (K) metrics. These indices are derived using the confusion matrix, see Congalton (1991). Global accuracy is a metric expressing the overall amount of correctly classified pixels, whereas Kappa measures the difference between the global accuracy of the model and the agreement expected by chance. For both modelling approaches, accuracy metrics were assessed against the set of validation points withheld from the overall dataset. Besides the statistical evaluation of accuracy, a visual assessment based on literature, expert and field knowledge was undertaken to investigate how well the produced thematic models represented reality and better address the previously mentioned points.

### 3.2.7. Observation and quantification of environmental variability

Three experiments were conducted to study environmental variability and its influence on high-frequency backscatter measurements (Montereale Gavazzi et al. 2019). The surveying principle designed to capture short-term backscatter variability over the same seafloor patch consists of a series of repetitive MBES measurements performed over the duration of a tidal cycle. The same reference survey-line (~2 km) was followed using the same heading and crossing the centre of a region of interest (ROI) of approximately 500x200 m for the first two experiments, situated in the Westdiep and Kwintebank areas, and 200x50 m for the third one, situated in the MOW1 area. Each experiment consists in the acquisition of a short-term backscatter and bathymetry time series according to the described strategy. To interpret the acoustic data, different strategies were put forward to quantify environmental variables during the experiments. For the oceanographic instrumentation employed in the experimental methodology see §3.1.1.

Different products were derived from the Kongsberg datagrams by using different software tools. All BS data were taken within the selected ROIs. Using the SonarScope© software suite, time series of Angular Response (AR) curves were derived from the beam intensity datagrams. The seafloor angular backscatter strength is computed from the following sonar equation liking the transmitted and received signal levels with the transmission losses and the backscattering process:

$$EL\,(R,\theta) = SL - 2TL\,(R) + 10\,log\,A\,(R,\theta) + BS\,(\theta),$$

where EL is the Echo Level (referenced to 1 µPa) measured at the receiver as a function of the sonar-to-target range R and the angle of incidence Θ of the signal onto the seafloor, SL is the Source Level, 2TL is the two-way Transmission Loss accounting for both geometrical spherical spreading and absorption (see Francois & Garrison 1982a, 1982b), A is the instantaneously insonified area, delimited by the MBES beam aperture and/or signal duration, and BS is the Backscatter Strength of the seafloor target at the observation angle Θ. The data reduction scheme relating to the AR datatype (Table 4.4 in Montereale Gavazzi 2019) is despite being relative, considered to be the best estimate of the raw BS angular response (Fezzani & Berger 2018; Roche et al. 2018).

Different mechanisms beyond the inherent geometrical (spherical) spreading of the sound wave control the attenuation during the propagation in seawater and can be responsible for unwanted signal fluctuations and degradation of the signal-to-noise ratio (Lurton 2010). Particular attention has been placed on the quantification of 2TL transmission losses resulting from hydrological conditions of the sea water. Overall, attenuation losses result from the contributions of: (1) absorption in clear seawater (αw, see Francois & Garrison, 1982a, 1982b); (2) viscous absorption (αv, see Urick 1948); and (3) scattering due to the presence of SPM (αs, see Richards et al. 1996; Hoitink & Hoekstra 2005). The uncertainty introduced by the attenuation of sound in seawater only was estimated for each experiment for nadir (0°), oblique (45°) and fall-off angular regions (70°). For the second experiment, the absorption model by Francois & Garrison (1982a, 1982b) was applied to the set of water-column profiles obtained by the CTD frame down-casts; for the two other experiments, only surface values of absorption coefficient were considered. Using the modelling approach by Richards et al. (1996) and Hoitink & Hoekstra (2005), sound absorption due to presence of SPM was estimated for the second and third experiments. For the second experiment, this uncertainty was estimated for the 1m profile above seafloor using the vertically averaged ABS-derived SPMC and median particle size (D50). Additionally, uncertainty was estimated along the quasi-continuous sediment profile (~15 m depth) that was reconstructed combining observations from the various sensors. To appraise the effect of particle size, the D50 of the lower part of the profile was altered from 100 to 400 µm reflecting the sand particles potentially resuspended in the near bed of this area during maximum currents. Despite a lack of data to carry out a similar analysis in the third experiment, the available OBS-derived SPMC time series were coupled to the MBES BS by means of correlation analysis. Nonetheless, similarly to the second experiment, the effect over the full water depth was estimated by reconstructing a quasi-continuous sediment profile based on SPMC from the OBS and using a fixed D50 of 63 µm. The effect of particle size was investigated by changing the D50 of the lowest part of the profile from 63 to 125 µm, approximating to the fine sand observed in the grab samples.

A pre- post and ensemble methods classification were performed on the backscatter time series in order to extract trends and patterns of change in substrate classes (Montereale Gavazzi et al. 2018). Ensemble approaches combine supervised and unsupervised classifiers, whereas a pre-classification method focuses on the unclassified data values. The aim of a post-classification approach is to allocate class labels to the data values to produce thematic maps. These change detection methods are based on the previously described approaches of predictive modelling and error estimation. The pre-classification approach uses backscatter values taken from rectangular bins of the sampling locations representative of the different geomorphological and substrate features of the ROIs. Following, basic statistics and temporal trends were studied (Hammerstad 2000). In order to detect outliers in the time series, sigma detections where chosen as the favoured statistical measure to quantify the dispersion of a set of data values. An ensemble method, combining supervised and unsupervised classifications was also applied. The K-means classes identified in a ground-truth time series were used to reclassify the complete dataset for which ground-truth data were not available. From this classified dataset, proportion counts were extracted to observe temporal trends. Prior to transforming the successional backscatter mosaics into classified data, the Within Group Sum of Squared Distances was computed independently for each dataset. This technique is similar to computing a silhouette plot where the optimal number and size of classes in a dataset becomes visible (Montereale Gavazzi 2019, Ch. 3). The post-classification approach made use of the transition matrix (Pontius et al. 2004; Braimoh 2006; Rattray et al. 2013). In this analysis, two unsupervised seafloor maps (e.g. prior and after a natural or anthropogenic event) are cross tabulated to derive detailed statistics describing the temporal changes. Persistence and class swap dynamics, gross gains and losses, between time and between classes' transitions, as well as persistence ratios expressing the tendency of a category to undergo a certain change process were derived after Braimoh (2006). Swap defines the change in spatial location of a substrate type between times. The net change describes the difference in quantity of a substrate class between times. Gain and Loss describe an increase and decrease of the areal extent of a substrate class respectively. The net change to persistence ratio indicates the overall trend of a category with negative and positive values indicating the directionality of the temporal trends.

## 3.3. Bed shear stress

### 3.3.1. In situ measurements of bed shear stress

The bed or bottom shear stress determines the erosion and resuspension of the material or the deposition of the material on the sea bed and is as such the link between the material in the water column and the material on the sea bed. Bottom shear stress cannot be measured directly and has to be determined indirectly from current profiles or high frequency velocity measurements. A method based on current profiles and three other ones based on high frequency velocity measurements (Lecouturier 2000; Giardino & Monbaliu 2006) have been applied and validated with our data.

Long-term measurements of high frequency velocity and current velocity profile measurements are available from 2005 onward for the Belgian part of the North Sea. The measurements were executed with benthic lander (tripod) equipped, amongst others, with a SonTek ADV Ocean point velocity meter measuring at 0.18 m above the bed (mab) high frequency current velocity. The downward looking SonTek 3 MHz ADP current profiler, installed at 2.3 mab, measures the near bed current profile with a resolution of 0.1 to 0.15 m. Additionally a bottom mounted Acoustic Doppler Current Profiler (ADCP), type Sentinel 1200 kHz Workhorse, has been used to register the currents over the entire water column. During the period 2005-2019 more than 120 deployments with the tripod have been executed. Most of them are located at the station MOW1 in the coastal turbidity maximum zone about 5 km northwest of the port of Zeebrugge. Other locations are Blankenberge, MOW0 and WZ-buoy, all three also situated in the coastal turbidity maximum zone. Other deployments are located more offshore, i.e. Gootebank and Blighbank.

### *Current profile method*

The current profile method uses the current profile, measured by a profiling current meter (ADP or ADCP). The bottom shear stress is calculated assuming a logarithmic profile of the current near the bed, which is valid in the lowest 20% of the water column, below the outer turbulent region (Wilcock 1996). The measured profile is fitted to this logarithmic profile using a least squares method (Wilkinson 1984; Drake et al. 1992). Furthermore Wilkinson (1984) developed expressions for the confidence limits for the estimations of the bottom roughness length and the bottom shear stress, using the Student’s t distribution for the number of freedoms, equal to the number of velocities minus 2. The actual profiles may differ significantly from the averaged profiles (Gross et al. 1992).

### *High frequency velocity methods*

The available ADV data set consist of about 7500 burst samples of the 3D velocity components measured at a sampling frequency of 25 Hz and an interval of 15 minutes. Besides the velocity components, the ADV records the correlation between the three beams, which is a measure of the data quality. Data quality can be influenced by e.g. bubbles or suspended sediments (Elgar et al. 2005). According to the manual of the instrument, data are suspicious when the correlation falls below 70 %. The data analysis starts with removing the bad or suspicious bursts. This is done if more than 5% of the data have a correlation of 70% or 80 %. In the second step spikes in the data are removed following the method of Goring & Nikora (2002). This method says that the original data and the first and second derivatives plotted against each other in a space-phase plot that fall outside the ellipsoid defined by the universal criterion are designated as spikes. These spikes are replaced by a third order polynomial using 6 points on either side of the spike. The method re-iterates until all spikes are removed.

#### Reynold stresses or eddy correlation method

The first method calculates the bottom shear stress from the total Reynold stresses (e.g. Huthnance et al. 2002; Williams et al. 2003). This method is easy to apply, but the calculations are very sensitive to the correct vertical alignment of the velocimeter (Huntley 1988; Dyer et al. 2004; Inoue et al. 2011). In theory, waves do not contribute to Reynolds stresses because the horizontal and vertical components of the wave-currents are 90° out of phase. However, if the vertical alignment is not correct, horizontal velocities can leak into estimates of vertical velocity and vice versa. Different methods are used to correct for this misalignment (e.g. Elgar et al. 2005). Kim et al. (2000) have suggested to rotate the coordinate system first around the vertical axis until the mean flow is zero along one horizontal axis and afterwards around this horizontal axis until the mean vertical velocity is zero. Another method to remove the effect of the waves on the Reynolds-stresses was proposed by Lohrman et al. (1995). They suggested to rotate the currents around the x- and y-axis until the mean vertical velocity is zero and the mean variance of the vertical velocity fluctuations is minimal.

Since the mean vertical velocity and the variance of the vertical velocity fluctuations are calculated for all combinations of rotations over the x- and the y-axis, this method needs much calculation time. Other methods to calculate the Reynolds stresses have been proposed that uses the different along-beam velocities of the ADV (Stacey et al. 1999; Fugate & Chant, 2005; Nystrom et al., 2007). Walter et al. (2014) have proposed a method that uses a spectral phase decomposition to separate the turbulent and the wave part in the Reynolds stresses.

### Inertial dissipation method

The inertial dissipation method relates the shear velocity to the energy dissipation, which is calculated from the velocity spectrum (Huntley 1988; Sherwood et al. 2006). In the power density spectrum, a region exists, the inertial subrange, where the three-dimensional spectrum of turbulent motions $E(k)$ is scaled by the turbulent dissipation rate $\varepsilon$ and decreases with the three-dimensional wave number $k$ at the characteristic -5/3 slope. The turbulent dissipation is calculated from a transformed spectrum in a frequency range (typically between 1 Hz and 2.5 Hz) not disturbed by the instrument noise, at higher frequencies. The spectrum is further corrected with a factor to account for the presence of waves (Trowbridge & Elgar 2001; Sherwood et al. 2006). In this method, the turbulent dissipation is calculated from the frequency region, where the slope of the transferred spectrum is closest to zero, i.e. the frequency region where the -5/3 decay rate is the closest followed. Using the turbulent dissipation, the bottom shear stress is then calculated from a relation that also includes the height above the bottom. This is at the same time the main disadvantage of this method. To calculate the height above the bottom, where the measurements have been executed, the altimeter of the ADV is used. Remark that the normalised power density spectrum of the vertical velocity is used, since this is generally less disturbed by noise. More information on the implementation of the method can be found in Francken & Van den Eynde (2010). Remark that the detrending of the data, before calculating the power density spectrum, results in a slightly higher bottom shear stress, when the inertial dissipation method is used, due to the normalisation of the power density spectrum to the variance of the data.

### Turbulent kinetic energy method

The third method calculates the bottom shear as a linear function of the total turbulent kinetic energy, which is calculated from the variance of the velocity fluctuations. The proportionality factor C is equal to 0.19, as proposed by Stapleton & Huntley (1995) and Thompson et al. (2003). The advantage is that this method is straightforward to apply. However, the turbulent kinetic energy, is not only influenced by turbulence but also by the prevailing waves. Typically, between 1/6 Hz and 1/25 Hz an increase in the power density spectrum of the velocity can be observed with a characteristic well-known -5 power decay, typically for wave spectra. Different methods are available in literature to split the two spectral densities, e.g. Soulsby & Humphery (1990). To calculate the power of the turbulence, the power spectral density is interpolated across the base of the wave peak. By doing so the bottom stress, calculated using the total turbulent kinetic energy, corresponds to the maximal bottom shear stress under the influence of currents and waves, while the bottom stress, using the turbulent kinetic energy, after removal of the wave and long-period variations, is a measure of the mean bottom stress under the influence of the waves and the currents (Verney et al. 2007; Verney 2008). This mean bottom stress is comparable with the bottom shear stress, calculated with the inertial dissipation method, from the Reynolds stresses and from the velocity profile.

### 3.3.2. Classical modelling of bed shear stress

Different methods and techniques have been described in literature of various complexity to model the bed shear stress. This also applies to the bottom roughness length, one of the main parameters that determines the bottom shear stress. All these different models can give results that can vary over a large range. While in the next paragraph (§3.3.3), more elaborate and developed state-of-the-art methods for the calculation of the bottom shear stress are proposed, using new insights in the physics of the near bed layer, in this paragraph, some more classical and widely-used methods are described These classical methods to model the bottom shear stress have been used to evaluate the bottom shear stress measurements described in the previous paragraph.

#### *Modelling bottom shear stress*

The (classical) bottom shear stress calculations under the influence of currents alone or waves alone on a rough bottom is well described in literature. The bottom shear stress under the influence of currents can be described as a function of the depth-averaged current or as a function of the current at a certain height above the bottom. The bottom shear stress under the influence of waves is described as a function of the wave orbital velocity near the bottom. In Van den Eynde & Ozer (1993), different simple models were compared with each other and with the results of more complex model, as presented in Dyer & Soulsby (1988) and Soulsby (1995). The Soulsby (1995) formulae are the results of a two-coefficient optimization of a simple model to 131 data points, from more complex theoretical models. Soulsby & Clarke (2005) developed a new model, assuming an eddy viscosity varying over the water column, but constant in time. The eddy viscosity varies linearly above the bottom in the thin wave boundary layer and has a parabolic function outside the wave boundary layer. Remark that the eddy viscosity is much higher in the thin wave boundary layer than outside. Furthermore, the eddy viscosity in the wave boundary layer is only a function of waves and currents, so that no iterative calculations are needed. In the wave boundary layer, the shear stress is constant, outside the wave boundary layer, the shear stress varies linearly, to zero at the water surface. A current profile can be calculated, integration of the current profile over the water depth results in the depth-averaged current, a quadratic equation is then used to solve for the bottom shear stress. The model of Soulsby & Clarke (2005) gives both a formulation for the maximal bottom shear stress during a wave cycle, and the mean bottom shear stress averaged over a wave cycle. The model was developed for flow over rough and smooth bottom. Malarkey & Davies (2012) further developed the theory of Soulsby & Clarke (2005) to include additional non-linearity in the model, which is present in the more complex theoretical models.

The bottom roughness length, i.e. the height above the bottom were the logarithmic current profile becomes zero, is a function of the grain size of the bed material, the ripples and the bed load. Instead of using the bottom roughness as a tuning parameter, the bottom roughness length can be calculated independently as well. The skin bottom roughness is mainly a function of the median grain size of the bed material. Different models have been implemented to calculate the bottom roughness due to bed load (Wilson, Nielsen, Soulsby and Raudkivi described in Grant & Madsen 1982 and Soulsby 1997). The bottom roughness, due to ripples is based on Soulsby (1997), Grant & Madsen (1982) and Soulsby & Whitehouse (2005). The latter model has the advantage that is was validated against many laboratory and field experiments and that the time evolution of ripples can be accounted for.

#### *Numerical models for currents and waves*

For the calculation of the currents, the three-dimensional hydrodynamic modelling software COHERENS has been used. The model was developed between 1990 and 1998 in the framework of the EU-MAST projects PROFILE, NOMADS and COHERENS. The hydrodynamic model solves the momentum equations, the continuity equation and the equations for sea water temperature and salinity. The momentum and continuity equations are solved using the mode splitting technique. COHERENS disposes over different turbulent closures. A new version of the COHERENS software has been developed recently (Luyten et al. 2014), mainly allowing the model to use parallel computing, while adding also some new features, such as improving the numerical scheme and adding a wetting-drying mechanism. The model OPTOS-BCZ is based on COHERENS and covers the Belgian Continental Shelf with a grid resolution of 42.8” in longitude (816 to 834 m) and 25” in latitude (771 m). This model has 10 σ-layers distributed over the total water depth. Along the open boundaries, the model is coupled with two regional models. The OPTOS-CSM model comprises the entire Northwest European Continental Shelf and calculates the boundary conditions of the North Sea model OPTOS-NOS. The latter calculates the boundary conditions of the OPTOS-BCZ model. The OPTOS-CSM model calculates depth-averaged currents and is driven by the water elevations at the open sea boundaries, using four semi-diurnal and four diurnal constituents. The OPTOS-BCZ model has been validated, amongst others, by Van Lancker et al. (2004), Dujardin et al. (2010), Mathys et al. (2011) and Van den Eynde et al. (2014).

For the calculation of waves, the WAM model has been used. WAM is a third-generation wave model, developed by the WAMDI Group (1988) and is described by Günther et al. (1992). It includes ‘state-of-the-art’ formulations for the description of the physical processes involved in the wave evolution. In comparison with the 2nd generation model, the wave spectrum has no restrictions and the wind sea and the swell spectrum are not treated separately. The model runs on three coupled model grids. A coarse model grid comprises the entire North Sea, the fine one the central North Sea and the local one calculates the waves in the Southern Bight. The local model has a grid resolution of 0.033° in latitude and 0.022° in longitude. The WAM model was validated by Van den Eynde (2013).

### 3.3.3. New developments in modelling of bed shear stress

A detailed theoretical study has been made on the determination and use of the bed shear stress in numerical models for hydrodynamics, waves and morphodynamics in coastal areas, including a critical review of the literature on this topic. Implications regarding the experimental determination of bed shear stress (cf. §3.3.1) are also analysed.

#### *Bed shear stress under steady currents*

The first part of the study deals with the bed shear stress under steady, i.e. equilibrium, conditions. While these conditions are rarely encountered in the field, this study is important since it forms the foundation for most of the theories that are applied in both numerical modelling and in measuring techniques. The bottom shear stress is often imposed as a bottom boundary condition in numerical models. This requires a closure which relates the bed shear stress to the flow field above the bed. This is realized by the friction law. The traditional friction laws are determined for steady flow conditions. However, imposing the bed shear stress as boundary condition implies equivalently that the velocity gradient is imposed. Without a reference velocity, it does not allow to predict the correct net flow field. This was confirmed and demonstrated by a simple steady pressure gradient driven 1DV open-channel testcase, where the COHERENS model produced very different velocities for different mesh structures.

A review is presented of the major friction laws for each of the hydraulic regimes: laminar, hydraulic smooth and hydraulic rough. Subsequently, a critical review is made of the different predictors of roughness height, providing insight in its definition in the case of very rough conditions, as it introduces the problem of the proper definition of the actual level of the bottom where the velocity becomes zero. This distance to the bottom is crucial for the bed boundary conditions for velocity and turbulence (eddy viscosity, turbulent kinetic energy, turbulent dissipation rate), which all rely on mixing length theory, where the distance to the wall is the key parameter. Due to the large gradients in velocity and turbulent dissipation rate, the sensitivity to the right wall distance is very large and quickly introduces errors. This is enhanced by the fact that the solutions in the nodes of the numerical grid are in most used software packages interpolated linearly.

The latter problem has been further investigated and a new method has been developed to define alternative bottom boundary conditions: they are theoretically not exact, but they compensate for the errors generated by the linear interpolation and guarantee conservation of mass flux, a correct bed shear stress (i.e. momentum conservation) and conservation of turbulent kinetic energy. The method implemented in TELEMAC yields better results, but not good enough since the final result proves to be still influenced by errors in the layers above the wall layer. This problem needs further investigation.

The fact that the law of the wall is expressed in terms of the non-dimensional wall distance (also called wall coordinate) $z_+ = zu_*/\nu$ (where $u_* = \sqrt{\tau_0/\rho}$ is the shear velocity, $\tau_0$ the bed shear stress, $\rho$ the fluid density and $\nu$ the fluid viscosity) has generated a lot of misconceptions, in particular in the case where there is significant bed load transport. This has been investigated already for a long time by Toorman, using the unique experimental data for steady sand transport in a laboratory flume by Cellino (1998). Continuing on the earlier findings, the possibility has been investigated that the non-dimensional velocity profiles should be represented differently, by using not the properties of the suspending medium, but the density and effective viscosity of the total sediment-water mixture. This is the only way that the non-dimensional profile can fulfil the asymptotic behaviour $u_+(= u/u_*) = z_+$. The effective suspension viscosity is found to account not only for viscous effects, but also intergranular shear and collisional losses, and possibly turbulence by vortex shedding in the wake of particles. Unfortunately, the vertical resolution of the Cellino data is still not fine enough to extract the effective viscosity profile sufficiently accurate. Research at KU Leuven, support by MSc thesis projects in collaboration with DEME, on the pumping of homogeneous fluid mud suspensions has further confirmed the need to use the slurry viscosity (defined by a Bingham rheological closure) to non-dimensionalize the velocity profiles.

This study furthermore allows to shed new light on the ongoing discussion of the apparent decrease of the von Karman “constant” $\kappa$ due to sediment in suspension. It has now been demonstrated that the velocity profiles rather show a compression of the log-layer (without needing to reduce the value of $\kappa$ =0.4) by the apparent thickening of the inner boundary layer, while the deviations near the surface remain attributed to 3D effects of interference of bottom-generated turbulence with sidewall-generated turbulence (e.g. Yan et al. 2011), sometimes mathematically corrected by Coles’ “law of the wake”. More insight has also been gained in the understanding of apparent drag reduction by high concentrations of sediments. It can be understood from the fact that a plug flow (where the shear stress is smaller than the yield stress and the velocity gradient is zero) theoretically does not dissipate energy. Therefore, the thickness of the plug should not be included in the flow depth as length scale for the bulk Reynolds for a fair comparison. Pumping experiments, indeed show a systematic increase of friction losses with increasing density, i.e. increasing yield stress.

Most of this study focusses on the bed shear stress from a 1DV, 2DV or 3D perspective where vertical profiles are supposed to be known or computed. However, for reasons of computational efficiency, it remains important to also consider the implications for the bottom boundary conditions in the case of depth-averaged modelling. The removal of the vertical dimension requires a different, modified approach. The general classical procedure is to express the friction law in function of the depth-averaged velocity, for the simple reason that it is assumed to be linked to the shear velocity through the (integrated) logarithmic velocity profile. In a previous study, Toorman (2012) already extended this friction law to become valid over the entire range of hydraulic regimes: laminar to turbulent smooth and turbulent rough. It has successfully been used in an application the Scheldt and Belgian coast (Bi & Toorman 2015), where it yields significant better and more stable results in shallow and intertidal areas. The remaining problem of the explicit water depth predictor, which causes an undesirable time lag, has been investigated in a MSc thesis by Vereecke (2019), but no good solution could be found and further research is needed.

### *Bed shear stress under unsteady conditions*

In a second part of the study the bed shear stress and associated sediment transport under waves is studied. For this purpose, flume experiments are simulated with the recently developed MixtSedFOAM (Ouda & Toorman 2019)[1]. After calibration of the model with the limited flume data, the model results generate a lot of additional data in space and time, which allows a much deeper analysis than based on the lab data only.

An additional advantage of this modelling framework is its ability to include (a part of) the sediment bed in the computational domain. Subsequently, no friction law is required at the interface between water and bed. The actual stresses are now computed by the semi-empirical rheological closures for the sediment-water mixture. The data of these simulations are used to re-evaluate popular (semi-)empirical closures to estimate the (maximum) bed shear stress and net sediment flux by waves. Subsequently, it is aimed to develop improved parameterized closures for implementation in TELEMAC-TOMAWAC, where the wave field is resolved in the frequency space.

[1] MixtSedFOAM (Ouda & Toorman 2019) is a sediment transport module for OpenFOAM that solves the fundamental equations for sediment transport based on two-phase flow theory and then recombined to a mixture theory model. The resulting model can consider a lot more physics than traditional sediment transport models and is valid from dilute conditions up to high-concentrated sheet-flow and (approximately) motionless sediment beds. In order to well capture the large gradients near the water-bed interface, the model needs a fine computational mesh, resulting in a limitation of applicability to small scale problems. Therefore, this model will mainly be used as a numerical laboratory, as in the present case of wave-sediment bed interaction.

### *Implications for measurements*

An important consequence of the above study for bed shear stress measurements, is the fact that the traditional methods to compute the bed shear stress from vertical profiles of velocity, Reynolds stress or turbulent kinetic energy (TKE), which implicitly assume steady conditions, may be incorrect. The more dynamic the system, the more time lag one can expect between bed shear stress and mean flow velocity. This is exemplified by the case of bed shear stress under a sinusoidal wave, where there is a phase shift of 90° (based on the ideal potential wave theory). In addition, recent data from DNS simulations and from measurements in the Princeton super pipe facility have created doubt on the universality of the law of the wall and of the constants in well-known turbulence models (like the standard $k-\varepsilon$ model). For instance, these data indicate that the value of the parameter $c_\mu$ (usually taken 0.09) decreases with increasing Reynolds number. This implies that the assumed relation between TKE and Reynolds stress may no longer be valid and could imply that the TKE method is the least reliable. Nevertheless, the shape similarity between TKE and Reynolds stress has been verified for the Cellino data (assuming that the missing spanwise TKE component can be estimated as 1/3 the streamwise component, based on the work of Nezu & Nakagawa (1993), and proves to yield quite good agreement. But this is of course only valid for steady flow conditions. A critical review for unsteady conditions will follow from the PhD research of Zhang (2020).

# 4. SCIENTIFIC RESULTS AND RECOMMENDATIONS

## 4.1. Uncertainty in measuring the indicators

### 4.1.1. SPM concentration and particle size measurements

#### *SPM concentration and turbidity*

The benefits and limitations of using optical and acoustical backscatter sensors to acquire long-term observations of SPMC and the formulation of recommendations on how to best acquire quality-assured SPMC data sets, based on the challenges and uncertainties associated with those long-term observations as well as the means to quantify and reduce the uncertainties associated with SPMC measurements was published in Fettweis et al. (2019), as a task of the project. The overall error of the SPMC data set consists of random errors that lead to uncertainties of individual SPMC but approximate the accurate value with increasing amount of data, and of systematic errors (biases) that lead to an average over- or underestimation of all data. Some errors can be detected, and to some extent corrected, whereas, others are inherently associated with the applied technologies and its interference with the environment and remain spurious and difficult to quantify or to control. The first types of errors are related to the sensors, sampling and lab protocols or the modelling techniques, while the latter are mainly related to systematic, often gradually changing natural variability in SPM inherent properties.

To separate variability due to measurement errors from variability due to natural variations in inherent optical properties of the SPM, protocols that use the same water sample for filtration and for turbidity estimation should be used in parallel to the in-situ procedures. Despite calibration to a formazine reference solution and the use of ISO-normed optical sensors, model calibration may vary considerably in recorded turbidity for a same SPMC solution across different instruments resulting in instrument-specific turbidity-SPMC relations. Although different types of optical sensors have been calibrated against the same reference solution, they yield up to 20% differences in the field. These results prohibit the comparison of turbidity values measured by different types of optical sensors. Turbidity as a surrogate of SPMC is thus only reliable, as long as site-specific (model) and instrument-specific (sensor) calibrations are carried out.

Optical and acoustical sensors have proved invaluable in the study of SPM dynamics in marine and estuarine environments as they allow collecting easily in situ, high-frequency SPMC time series over long periods of time. The payback is the availability of large homogeneous data set of SPMC from various locations on the globe; the drawback is that the quality or certainty of the data and thus also the inter-comparability depends on factors that are only to a certain level avoidable. Long-term observations of SPMC are the result of a complex ladder of operations that involve field, laboratory and modelling methods. Each step contributes its own random and systematic errors to the overall uncertainties of the sensor SPMC. Systematic errors related to the functioning of the sensors, the environment, the collection and processing of calibration samples and faulty human operations are detectable and sometimes correctable. As long as protocols for sample analysis and sensor calibration are carefully followed, uncertainties can be confined within ±5%, otherwise they may reach up to ±20%. Biofouling may add a further bias of 100% (positive for optical, negative for acoustical sensors), and their detection generally leads to a loss of data. A good understanding of the processes that are causing changes in SPMC and particle inherent properties (size, shape, density and composition) is required in order to estimate their importance and to possibly rescale the sensor data to some reference particle properties. Variations in these properties may result in over- or underestimation of the SPMC by up to a factor 2 or more. Based on the uncertainties, listed in table

3 of Fettweis et al. (2019), one can achieve random errors below 25% and biases below 40% only with substantial efforts in technologies that indicate the changes in inherent particle properties.

Acoustical and optical sensors require both the conversion of the sensor output (after sensor calibration) to a mass concentration. This is done by relating the sensor output to a reference SPMC, which is preferably the sample SPMC. The choice of the regression method, the dependent and independent variable, and the error associated with the reference SPMC determines the coefficient of determination. In Fettweis et al. (2019) a model was built that based on the $R^2$ and the normalized turbidity/dB quantifies the uncertainty of the sensor derived SPMC in the calibration range and outside of it. The model shows that the Robust fit (iteratively reweighted least squares regression) and the Eigenvalue regression have less prediction bias than the Theil-Sen estimator and the ordinary least square regression. This bias is not an issue for $R^2>0.9$ and remains below 10%, but it becomes significant for lower $R^2$ and can amount to 30%. Short-term variabilities in the model-regressions generally show up as random noise limiting the $R^2$ of the calibration data set, but the extrapolation of the regression parameters to longer periods or larger areas may introduce biases of more than 50%.

### *Particle size measurements*

The different methods that are used to measure in situ particle size distributions (PSD) may not give the same results. A PSD measured by a LISST will differ from the one measured by a digital camera (e.g., Mikkelsen et al., 2005), meaning that the outcome of even the best flocculation model is only as good as the measuring system that is used to collect the FSDs. The uncertainties associated with a measuring technique are related to the characteristics of the particles occurring in nature (Mikkelsen et al. 2006; Andrews et al. 2010; Davies et al. 2012; Graham et al. 2012), and to the measuring principle itself (Mikkelsen et al. 2005; Goossens 2008). Generally, camera systems cannot resolve the fine particles smaller than 10 µm, while LISST has a limited size range for the fine and the very large particles. Out of range particles are influencing the size distribution of the LISST. For example, particles smaller than the size range of the LISST affect the entire PSD (Andrews et al. 2010; Graham et al. 2012). A rising tail in the lowest size classes of the LISST is frequently observed in our data and is interpreted as an indication of the presence of very fine particles rather than providing a correct number. Particles exceeding the LISST size range of 500 µm also contaminate the PSD. Davies et al. (2012) reported that large out of range particles increase the volume concentration of particles in multiple size classes in the range between 250 and 400 µm and in the smaller size classes and recommended to interpret the PSD with care in case particles outside the size range may potentially occur. The importance of these spurious results depends on the number of large particles in the distribution (Davies et al. 2012). Nowadays, there is still no good way for correcting PSDs for these spurious data, but we should be aware that the very large (megaflocs) and the very small particles (primary particles) maybe under-represented or over-represented in the in situ LISST derived PSDs. Despite the uncertainties and limitations of the LISST-100C, it is well suited to collect long-time series of PSD autonomously.

Even if the size distributions of flocs are well resolved, there are still uncertainties involved in the estimation of the density and the settling velocity, the latter being the ultimate parameter for numerical models. To investigate settling velocity dynamics, estimates of floc size and floc density are required. In literature, the fractal theory is commonly used for relating floc size and floc excess density (Kranenburg 1994; Chen & Eisma 1995; Dyer & Manning 1999). Small changes in fractal dimension may induce large changes in the settling velocity. A sensitivity analysis of the fractal approach to model floc density has been described in Chapalain et al. (2019). In the fractal model, primary particles are characterized by a unique size and density and it is generally assumed that a floc only includes mineral particles whereas particulate organic matter (OM) is not considered (Khelifa & Hill 2006; Maggi 2013). However, these assumptions must be questioned as the primary particle size may vary spatially and temporally within the same area (Fettweis 2008; Maggi 2013), as biological or biomineral aggregates are ubiquitous in shelf seas and estuaries (e.g. Maggi 2009; Fettweis & Lee 2017; Shen et al. 2018b), and as the density of primary particles may change with changes in the composition of the SPM (Markussen & Andersen 2013). Our analysis also confirms that the application of the fractal approach, i.e. flocs are built from a unique type of primary particles characterized by constant size and density, has limitations. Also, depending on the history of flocs (eroded from beds, dynamically formed in the water column), flocs of similar sizes might be characterized by different densities (Smith & Friedrichs 2011), hence SPM could be subdivided into populations that might follow different fractal behaviours depending on their origin. Only very recently, few studies have discussed about the fractal theory. Fall et al. (2018) have demonstrated that there is not necessary a unique relation between floc size and excess density but that the fractal approach could be valid for floc sub-population, such as macroflocs or megaflocs.

### 4.1.2. Seabed/habitat type

#### *Acoustic Seafloor Classification*

Two major topics were researched: (1) the study and validation of sediment-acoustic relationships in a field/operational setting, enhancing the interpretability of high-frequency backscatter measurements based on readily accessible substrate characteristics from the available ground-truth data. This aspect therefore intended to provide researchers and end users a realistic perspective on what the MBES acoustic data can represent in terms of predicting material properties of the seafloor using conventional ground-truthing approaches. (2) Automatic seafloor classification and thematic mapping of seafloor substrate type. The following key research findings were identified. Demonstration of a pragmatic field-based-solution (stable and monitored at-sea reference area, see Roche et al. 2018) to merge seamlessly disparate MBES backscatter datasets: a global challenge faced by the seafloor mapping community. It was shown that where compensated backscatter imagery is corrected for the angular dependence using angles (or average values from a range of angles) beyond 40°, the effect of sub-beam-topographic-roughness polarization will be cancelled out, allowing seamless merging of sediment-type datasets acquired in disparate azimuthal orientations. Using the available ground-truth data, and based on exploratory data analysis, a number of insights were gained in sediment-acoustic relationships. At the level of the sample loci, moderate to strong univariate associations were found between backscatter intensity and the percent weight of individual grain-size fractions, within mostly heterogeneous substrate types; and median grain-size diameter (D50), within relatively homogenous and unimodal siliciclastic substrate types. For the entire study area (i.e. the overall merged and seamless survey), moderate to strong associations were found by multivariate statistical analysis, as well as when considering each study area in isolation. This suggests that different sediment parameters explain the backscatter collected at different locations. Importantly, it is observed that while Folk thematic classes are a good global descriptor of backscatter variability, a strong degree of dispersion (in terms of backscatter values and basic statistics) exists for heterogeneous sediment classes causing the reduction of the information content (by class amalgamation), and the subsequent generalisation of the depiction of the seafloor's spatial structure, achievable by thematic classification using geologically-conceived classification schemes (here referring to Folk, 1954 and from there originated, EUNIS classification). Here, a clear trade-off between backscatter discrimination potential (dictated by frequency) and sediment classification scheme, and thematic accuracy and resolution, was identified, shedding novel insights into the future research objectives and steps that have to be taken in order to improve this current limitation (see Montereale Gavazzi 2019, Ch. 6). In the absence of a multi-parametric ground-truth sample description (first step in the classification process, see Fig. 2.14 in Montereale Gavazzi 2019), statistically relevant geomorphometric variables were found to significantly improve the statistical and spatial accuracy of the modelled sediment classes. Comparing unsupervised (partitive clustering classification) and supervised tree-based machine learning classification), it was found that the latter supersedes the former in all aspects when considering the "goodness of mapping"; i.e. thematic accuracy, spatial uncertainty, relevance of the contributing variables and validity of the geo-sedimentological patterns depicted in the final product. Lastly, clear trade-offs between number of sediment classes and scheme and thematic accuracy were detected, providing important considerations that can be of interest to seafloor mappers farther afield.

### *Observation and quantification of environmental variability*

Methodologies were set up to observe and quantify environmental factors of variability and how their short-term (referring to half-diel, tidal variations) cyclicity would affect the interpretation of single and repeated backscatter surveys. This highly experimental research, published in Montereale Gavazzi et al. (2019), endeavoured studying, observing and quantifying seafloor MBES backscatter variability for different seafloor areas that is due to short-term environmental cyclicity (i.e. tidal cycles). This research was intended to identify the sources and magnitudes of variability and therefore to provide surveyors and end-users with an improved understanding of how data, recorded in situ, be affected by such factors and subsequently, how to identify and deal with unwanted (external, to be filtered out) and/or intrinsic (characteristic of a given seafloor setting) sources of variability. Furthermore, the research provides important insights on how to set-up such experiments, highly relevant to the utilisation of seafloor MBES backscatter in the operational environment, where environmental monitoring is ultimately targeted. Understanding how the environment influences the measurements against the resolution needed to detect true seafloor changes, is a critical first step towards the implementation of monitoring strategies that use such a technology. Montereale Gavazzi et al. (2019) details an experimental set-up needed to quantify sources of environmental variability, providing a solid basis to conduct future experiments within predominantly muddy, sandy and gravelly seafloors. Similarly to the previous research aspect, this paper demonstrated how standardising operational procedures, in terms of acquisition and processing, allows comparability, and therefore a better exploitation of repeated measurements, particularly in view of absolute system's calibration. The analyses concluded that different seafloor and hydrodynamic settings vary considerably differently, and the backscatter measurements therein logged accordingly. The sources of variability identified refer to: polarization of sub-beam topographic roughness, hydrological conditions of the water medium (i.e. presence of suspended particulate matter and of salinity and temperature gradients) and seafloor mobility (i.e. near-bed sediment transport, processes of cyclical erosion/deposition). With regard to bypassing and/or correcting for the identified variability, methodologies have been implemented that allow the quantification of Transmission Losses (2TL), necessary to reduce the backscatter values to estimates that reflect the seafloor as oppositely to other processes (i.e. processes that need to be excluded when applying Acoustic Seafloor Classification and/or Change Detection). In Montereale Gavazzi et al. (2019) the implications of short-term variability on the use of MBES-measured BS for longer-term monitoring are identified and discussed, as well as whether such variability can hinder the detection of real seafloor changes by the backscatter measurement proxy-approach. The most prominent implications are; tidal periodicity and seasonality calling for careful consideration, especially in shallow areas with soft-material sediments and high sedimentary dynamics. Indeed, successive surveys of the same area may provide different information at various time scales (from day to year). In this regard, it is important that the tidal dependence (i.e. the oceanographic environment must be characterised in complement to the geophysical surveys) is analysed per MBES-BS time series. In a change detection framework using backscatter only and based on small Regions of Interest, spotting outliers (i.e. abrupt changes in sediment response) will be relatively straightforward in the clear water and stationary areas since the magnitude of the short-term variance remains within the envelope of sensor sensitivity as declared by the manufacturer (1 dB). On the contrary, the intrinsic “noisiness” (i.e. periodical variability) of the nearshore areas results in a potentially masking/blurring effect of changes in seabed type, introducing uncertainties due to the status of the water column (i.e. turbidity) or to the “mobility” of the water-sediment interface. Due to this, within such areas, the stability threshold must be defined contextually in accordance to the governing sedimentary environment, and a transition in seafloor status can only be detected from a trend analysis on a sufficient number of repetitive surveys. Direction and consistency of the trend, regardless of the noise envelope, can be a valuable proxy of change bypassing conflicting results from surveys acquired at different tidal and/or seasonal moments. The experiments demonstrated the sensitivity of seafloor backscatter to subtle seafloor changes that may be of interest in other applications, for example in monitoring sludge dispersal in respect to dredging and disposal sites, fish-farms and installation of anthropogenic infrastructures.

*Acoustic Change Detection*

Key research findings on acoustic change detection relate to the demonstration that stable and repeatable backscatter serial datasets, acquired within low-dynamic seafloor environments, allow an effective change detection. Where a paucity of samples exists for the entire MBES time-series dataset, but sufficient data are available for one single dataset, and where rigorous data acquisition and processing standards have been employed, the supervised and accurate information identified in one survey, can be confidently extended to the remainder of the time-series, allowing its full exploitation. The change detection methods applied showed that different change patterns of interest can be observed and quantified. Pre-classification allowed studying trends within well-defined portions of the seafloor (similarly to Montereale Gavazzi et al., 2019), whereas post-classification proved very useful to understand the broader picture: i.e. that of the entire study area. Post-classification is particularly recommended where issues of data rectification arise, by allowing the relative comparison of disparate datasets (e.g. the geographic delineations between 100 and 300 kHz datasets). Furthermore, this approach allows capturing important signals of change such as gross and net gains and losses, persistence and ratios to loss/gain of specific seafloor classes of interest.

### 4.1.3. Bed shear stress measurements

The different methods to derive the bed shear stress from current velocity measurements have been presented in §3.3.1. Not all the methods gave similar results when applied to our data sets.

### *Current profile method*

This method is not very robust, as the outcome is very sensitive to the number of velocity points that are included o calculate the logarithmic profile. Drake et al. (1992) used the logarithmic profile to calculate the bottom shear stress using only measurements at three levels above the bottom, we found that taking more data point decreases the confidence intervals and changes the calculated bottom shear stress by a factor 2 to 3. Furthermore, it was noted that the actual profiles may differ significantly from the averaged profiles (Gross et al. 1992). One of the reasons for this was that the current profile was disturbed by the measuring frame itself. Only 6% of the data had a coefficient of determination $R^2$> 0.95, while Drake et al. (1992) suggested to take only profiles with a $R^2$>0.997. Our results also indicate that velocity in the lowest bin, closest to the seabed, includes a lot of noise, possibly due to variations in bed level or to bed-load transport, which influences the bottom shear stress calculation. The values of the bottom stress obtained from this method are rather large, this could be due to effects of stable stratification associated with the occurrence of high SPMC (Kim et al., 2000; Fugate & Chant, 2005).

### *High frequency velocity methods*

As explained in § 3.3.1, the data analysis starts with removing the bad or suspicious bursts and with the removal of spikes from the data. In practice, only less than 1% of the data have been removed. During analysis of the ADV data we found that the burst length of the samples has to be long enough. During our first deployments a burst length of 400 samples was used, which was too short and the results were not reliable. Later the burst length was increased to include minimum 7500 samples, these data have been used in the analysis.

#### Eddy Correlation Method

Although the eddy correlation method is easy to apply, waves influence the results when the ADV is not perfectly horizontal. Two methods for rotation of the data have been applied. The rotation was calculated for the data within each tide and for the data within four successive tides. The rotation angles during each tide could change considerably and the obtained rotation angles were unrealistically high (up to 20°). Furthermore, the calculated Reynolds-stresses before and after rotation (calculated over four tidal cycles) did not decrease during periods with high waves. This is an indication that the method, applied to our data, does not give good results. Similar problems have been mentioned in literature and it is suggested that better estimates of the Reynolds stresses can be obtained when two ADV sensors positioned close to each other are used (Trowbridge 1998; Trowbridge & Elgar 2001).

#### Inertial dissipation method

The power density spectrum was calculated, using the de-spiked data and after detrending of the data, with 4096 points (i.e. for 2048 frequencies) and with overlap. The main disadvantage of the model is that it needs the height above the bottom, which is variable. Furthermore, the technique to remove wave influence is not very reliable.

#### Turbulent kinetic energy method

The method provides data of the maximal bottom shear stress during a wave cycle, and the mean bottom shear stress averaged over a wave cycle. Both results compare well with the model results.

*Analysis of the bottom stress measurements*

The bottom shear stress calculated with the different methods do not correlate very well with each other. For example, the bottom stresses derived from the current profile and the inertial dissipation method are significantly higher than those calculated from the Reynolds stresses or the turbulent kinetic energy. The influence of the waves on the bottom stress using the Reynolds stresses is obvious and is mainly due to a misalignment of the ADV. The Pearson’s correlation factor R between the bottom shear stress, calculated with the different methods varies between -0.2 and 0.8. The uncertainty in these results is therefore very high. During periods with higher waves, the correlation between the different results decreases further. It is clear that the different methods give quite different results. Given the difficulties with the bottom shear stress derived from the logarithmic profile and the Reynolds stresses, we expect that these estimates are less reliable. Also, the high values of the bottom shear stress obtained with the inertial dissipation method, makes this method less reliable. Our results suggest that the best results are obtained using the turbulent kinetic energy method.

*Correlation with modelling results*

To validate the measurements and the assumption that the turbulent kinetic energy method is the most appropriate one, we have compared the bottom shear stress derived from measurements with the one obtained in the numerical model results.

The correlation coefficient between the modelled currents and the ADP measurements vary between 0.76 and 0.80 and between the modelled and measured waves results is higher than 0.83. When comparing the modelled and measured bottom shear stress, best correlations are obtained with the measurements derived from the turbulent kinetic energy method, if the burst is long enough to obtain a reliable estimate of the power density spectrum. The overall correlation using all available data is 0.72, with a mean bias of 0.09 Pa and a RMSE of 1.14 Pa. In 88% of the available in situ data, the correlation is higher than 0.50. Remark that in the model a bottom roughness of 0.01 m has been used, this value of the bottom roughness is a tuning parameter to fit the model data to the measurements. Nevertheless, a bottom roughness of 0.01 m is a realistic value. Analysis of the model results further revealed that calculating the bottom roughness using the different models found in literature (see § 3.3.1), resulted in a too high value that did not improve the model results, but allowed the bottom roughness to vary in time due to prevailing currents and waves.

## 4.2 Uncertainty in modelling the indicators

### 4.2.1. SPM concentration and floc behaviour

The prediction of correct SPM concentrations is highly depending on the closure to compute the bed shear stress, i.e. the friction law used. Uncertainties on the bed shear stress (see §4.2.2) are thus transferred to uncertainties in SPM. A second important source of uncertainty is the determination of the bottom reference concentration. This is obtained from the empirical, and thus highly uncertain, bedload transport model for non-cohesive sediments. For cohesive sediments, one assumes that no bedload is needed, which is a misconception and ignores the formation of fluid mud in the inner boundary layer.

Furthermore, the vertical mass balance requires accurate prediction of the turbulent flux and the gravitational or settling flux. The latter depends on the settling velocity. The new flocculation modelling approach based on multi-class population balance equations increases the accuracy of instantaneous sediment fluxes significantly since it allows to account for spatio-temporal variations of the settling velocity and of the distribution of the sediments over multiple size fractions (floc populations). The turbulent flux requires a good turbulence model. However, it is well known that turbulence modelling remains the most challenging problem in computational fluid mechanics. In particular, for the present application, the important interactions between turbulence and suspended particles in the bedload layer require adapted boundary conditions for turbulence. Despite progress made, no generally applicable methodology could be finalized.

### 4.2.2. Physical based modelling of bed shear stress

The bed shear stress is an important bottom boundary condition that is computed from its relation to the flow field through a friction law. The major uncertainties are due to the very restricted validity of currently used friction laws:

- Defined for steady conditions only,
- Not properly taking into account energy dissipation by suspended sediments,
- Usually neglecting the spatio-temporal variations in bed forms,

An additional uncertainty follows from the numerical implementation which faces the introduction of errors from the linear interpolation functions that should approximate the non-linear profiles of the different variables.

## 4.3. Discussion, recommendations and conclusions

### 4.3.1. Relevance of indicators for ecosystem monitoring

#### *SPM concentration and turbidity*

Turbidity or SPMC are among the listed parameters to be monitored to quantify hydrographic conditions (descriptor 7), however no indicators or thresholds are yet designed. Any change in coastal management (dredged sediment disposal sites, sand mining, port developments, bottom trawling…) is expected to produce a change in the turbidity/SPMC, at the scale of the pressure and the surroundings. This research demonstrated that the actual monitoring strategies or protocols are adapted for tracking these changes statistically, as far as they are larger than the uncertainty range, i.e. 25%, and certainly lower if analysing trends.

#### *Bottom shear stress*

Bottom shear stress is a proxy of the energetic conditions a seabed or habitat is subdued to, hence relates to descriptor 7, i.e. hydrographic conditions (Belgian State, 2012). It links seafloor processes to the suspension capacity of the water column. Above certain critical thresholds a location may either be buried under depositing sediments when the average energetic conditions reduce, or washed away by erosion when the average energetic conditions increase.

#### *Seabed/Habitat*

Seabed/habitat type contributes to indicators on seafloor integrity (descriptor 6), see Belgian State (2012). This research showed that spatially-explicit monitoring using multibeam technology is possible when using standardized protocols for surveying, data acquisition and processing enabling the detection of changes and trends with a reasonable degree of certainty (Montereale Gavazzi et al. 2018; Montereale Gavazzi 2019). If extended regionally, and combined with other measurements and numerical models (e.g., sediment fluxes), results can provide evidence of larger phenomena of interest.

### 4.3.2. Recommendation and conclusions

*SPM concentration and turbidity*

Our study confirms that the relation between turbidity and sample SPMC is depending on protocols, technology and the manufacturer, and even may differ between sensors of the same type (e.g. Downing 2006; Rai & Kumar 2015; Rymszewicz et al. 2017). The relation between the output of an acoustical sensor and SPMC is even more variable. In spite of these uncertainties, turbidity is still often used as a proxy for water clarity or SPMC as is the dB of acoustical sensors. We advise to not use turbidity (or dB) for scientific purposes as it diminishes the comparability of the data. Instead, the sensor output should be transformed into a mass concentration, a unit that is comparable in time and between regions. If this is not possible, then the turbidity data should always be referred to the instrument used and the protocol applied. The problem aggravates when turbidity data that have been collected using different technologies and protocols over long periods of time and regional scales are stored in international data bases (e.g. turbidity in EMODnet, see http://www.emodnet.eu), and used to derive conclusive trends of the environmental status of marine and estuarine areas (Fettweis et al. 2019).

Monitoring in situ high frequency turbidity and SPMC is no longer an issue, considering that common guidance and protocols are applied to restrict their measurement uncertainties. However, in situ measurements from coastal observatories are still confined to local measurements and must not be considered alone but within a multi-source monitoring program. Hence local high frequency observations must be interpreted together with remote sensing ocean colour data, which provide daily synoptic surface turbidity/SPMC measurements, and numerical sediment transport model results, to assess the spatial extend of the pressure. The main challenge is now to evaluate model results uncertainty and improve the formulation of natural processes, together with the effects of pressures in the models.

*Bottom shear stress measurements*

Although different methods exist to derive estimates for the bottom shear stress from measurements, the application of these methods is not straightforward. Although promising results are found in literature (e.g. Lecouturier 2000; Allen et al. 2016), our results were not satisfactory. Low correlations were found between the bottom shear stress estimates using the different methods. Some possible reasons have been identified, but a careful analysis of the data did not improve the results. One of the main problems is that the modelling of the bottom shear stress as was done here is to pragmatic and lacks physical basis as is explained in § 4.2.2. Nevertheless, the bottom shear stress estimates using turbulent kinetic energy method are the most reliable ones. Given the relatively good correlation between modelled and TKE-based derivatives of bottom shear stress, we still find it appropriate to use bottom shear stress as an indicator supporting the MSFD descriptor hydrographic conditions.

*Seabed/Habitat type*

Following the procedures outlined in Montereale Gavazzi et al. (2018) and Montereale Gavazzi (2019), the indicators on seabed/habitat type can be mapped and monitored with a reasonable degree of certainty. Changes imposed by environmental cyclicity (tides and seasonality) can be accounted for following Montereale Gavazzi et al. (2019). To seamlessly map data from different surveys and different platforms, quality control and relative calibration of the acoustic data can be performed of which the procedure is outlined in Roche et al. (2018). To improve the detection of small-scale, though relevant ecosystem changes, centimetre-accurate depth measurements are recommended. Further research is needed on the optimal resolution of the classification and on most appropriate classification schemes addressing changes in seafloor integrity in higher detail. This requires multi-parameter ground truthing and increased sample size. Fostering multi-partner and regional cooperation is recommended to increase on the scale and frequency of the mapping. Mapping data, combined with other datasets, and results from ecosystem modelling, including data and modelling uncertainties, ideally combine into a multi-criteria assessment framework to understand cause- and effect relationships and propose appropriate measures preventing adverse biodiversity effects.

Some inherent limitations still exist when using multibeam-derived data products in MSFD/EIA reporting. These were listed in Belgium's 2018 MSFD assessment (Van Lancker et al., 2018), and were further elaborated in Montereale Gavazzi (2019). They relate to: (1) Complex sediment-acoustic relationships resulting in no uniform acoustic response per main seabed/habitat type. Variability is imposed by topographic roughness (including bioturbation), shell inclusions, various degrees of sediment porosity or compaction, dynamics of the water-sediment interface. Variability in heterogeneous seabeds, and gravel beds in particular, are difficult to detect because of other acoustic scattering regimes. (2) Data represent the top veneer of the seabed, making the data subject to temporal variability imposed by hydro-meteorological forcing. It also implies that smothering or siltation without significant surface expression cannot be detected. (3) Accuracy and/or error on the measurements only allows detection of changes of a higher order of magnitude. (4) State of the transducer varies over time and need accounting for. (5) Multibeam-derived data products alone do not allow distinguishing between naturally- versus human-induced changes.

# 5. DISSEMINATION AND VALORISATION

## 5.1. Organization of workshops

Final workshop of project "Developments of methods to improve the monitoring of MSFD indicators 6 and 7 (INDI67)", Brussels (Belgium), 19 June 2019.

Special session at GEOHAB 2018 on "Backscatter Working Group – Subgroup on Variability and Monitoring – BSWG-VARIMONIT ", Bremen (U.S.A, California, Santa Barbara), 7-11 May 2018.

SEACoP meeting on establishing a Community of Practice in 4D Seabed Mapping in Belgium, 23 June 2017, Brussels (Belgium).

Special session at ECSA 56 on 'Measuring bio-geophysical processes in dynamic and complex environments', Bremen (Germany), 4-7 September 2016.

Workshop on "Best practice in generating long-term and large-scale data sets of SPM concentration", Brussels (Belgium), 24-25 February 2016.

13$^{th}$ International Conference on Cohesive Sediment Processes (INTERCOH), Leuven (Belgium), 7-11 September 2015.

## 5.2. Participation at scientific and policy related meetings or conferences

The results obtained during the project have been presented at international and national scientific and policy-oriented workshops, meetings and conferences, a list of presentation can be found in Annex 1.

## 5.3. Support to decision making and applications

Results of the combined transect- and subregion-based monitoring, as reported under the theme Seabed/Habitat type, were further worked-out in the context of assessing seabed changes along the Belgian part of the North Sea. This forms part of Belgium's assessment of good environmental status of marine waters, as demanded by the European Marine Strategy Framework Directive (Van Lancker et al. 2018).

Seabed mapping results were also used in the framework of establishing baselines for future fisheries management (e.g. De Mesel et al. 2017). Additionally, based on recent seabed mapping results, the Habitat Directive area on the Vlakte van de Raan was redesigned and was incorporated in the revision of the Marine Spatial Plan. The SEACoP initiative on establishing a community of practice on seabed mapping is further elaborated by FPS Economy and Flanders Hydrography.

# 6. PUBLICATIONS

## 6.1. Peer reviewed publications


Chapalain M, Verney R, Fettweis M, Jacquet M, Le Berre D, Le Hir P. 2019. Investigating suspended particulate matter in coastal waters using fractal theory. Ocean Dynamics, 69, 59-81.

Chen P, Yu JCS, Fettweis M. 2018. Modelling storm-influenced SPM flocculation using a tide–wave-combined biomineral model. Water Environment Research 90, 244-257.

Fettweis M, Baeye M. 2015. Seasonal variation in concentration, size and settling velocity of muddy marine flocs in the benthic boundary layer. Journal of Geophysical Research, 120, 5648-5667.

Fettweis M, Lee BJ. 2017. Spatial and seasonal variation of biomineral suspended particulate matter properties in high-turbid nearshore and low-turbid offshore zones. Water 9, 694.

Fettweis M, Riethmüller R, Verney R, Becker M, Backers J, Baeye M, Chapalain M, Claeys S, Claus J, Cox T, Deloffre J, Depreiter D, Druine F, Flöser G, Grünler S, Jourdin F, Lafite R, Nauw J, Nechad B, Röttgers R, Sotollichio A, Vanhaverbeke W, Vereecken H. 2019. Uncertainties associated with in situ long-term observations of suspended particulate matter concentration using optical and acoustic sensors. Progress in Oceanography 178, 102162.

Montereale-Gavazzi G, Roche M, Lurton X, Terseleer N, Degrendele K, Van Lancker V. 2018. Benthic habitat change detection using MBES: Case study on the Belgian part of the North Sea. Marine Geophysical Research 39, 229–247.

Montereale-Gavazzi G, Roche M, Degrendele K, Lurton X, Terseleer N, Baeye M, Francken F, Van Lancker V. 2019. Insights into the short-term tidal variability of multibeam backscatter from field experiments on different seafloor types. Geosciences 9, 34.

Sahin C, Verney R, Sheremet A, Voulgaris G. 2017. Acoustic backscatter by suspended cohesive sediments: field observations, Seine Estuary, France. Continental Shelf Research 134, 39-51.

Shen X, Lee BJ, Fettweis M, Toorman E. 2018. A tri-modal flocculation model coupled with TELEMAC for estuarine muds both in the laboratory and in the field. Water Research 145, 473-486.

Shen X, Toorman EA, Lee BJ, Fettweis M. 2018. Biophysical flocculation of suspended particulate matters in Belgian coastal zones. Journal of Hydrology 567, 238-252.

Shen X, Toorman EA, Lee BJ, Fettweis M. 2019. Effects of aquatic biofilms on flocculation processes of cohesive sediments: A modeling approach. Journal of Geophysical Research 124, 4098-4116.

Shen X, Toorman EA, Fettweis M, Lee BJ, He Q. 2019. Simulating multimodal floc size distributions of suspended cohesive sediments with lognormal subordinates: Comparison with mixing jar and settling column experiments. Coastal Engineering 148, 36-48.

Toorman E, Fettweis M, Vanlede J. 2019. Editorial to the topical collection INTERCOH 2015. Ocean Dynamics.


## 6.2. Other publications

### 6.4.1. Theses


Chapalain M. 2019. Dynamique des matières en suspension en mer côtière : caractérisation, quantification et interactions sédiments/matière organique. PhD thesis, Université de Bretagne occidentale, Brest (France). 292pp + app.

De Bisschop J. 2016. Influence of water column properties on multibeam backscatter. MSc thesis Ghent University –Royal Belgian Institute of Natural Sciences, 74 pp.

Montereale Gavazzi, G.O.A, 2019. Development of seafloor mapping strategies supporting integrated marine management: application of backscatter by multibeam echosounders. PhD thesis, Ghent University, Ghent (Belgium), 392pp.

### 6.4.2. Proceedings and other publications

EuroGeoSurveys Marine Geology Expert Group. Annual Report 2017.

Papili S, Jenkins C, Roche M, Wever T, Lopera O, Van Lancker V. 2015. Influence of shells and shell debris on backscatter strength: investigation using modeling, sonar measurements and sampling on the Belgian Continental Shelf. In: Seabed and Sediment Acoustics: Measurements and Modelling, ed. by Blondel et al., 37, 304-310, University of Bath, Bath, Institute of Acoustics. Proceedings of the Institute of Acoustics.

Roche M, Baeye M, De Bisschop J, Degrendele K, De Mol L, Papili S, Lopera O, Van Lancker V. 2015. Backscatter stability and influence of water column conditions: estimation by multibeam echosounder and repeated oceanographic measurements, Belgian part of the North Sea. In: Seabed and Sediment Acoustics: Measurements and Modelling, ed. by Blondel et al., 37(1), 74-84, University of Bath, Bath, Institute of Acoustics. Proceedings of the Institute of Acoustics.

Van den Eynde D, 2016. Measuring, using ADV and ADP sensors, and modelling bottom shear stresses at the MOW1 site (Belgian continental shelf). Report MOMO-INDI67/1/DVDE/201608/EN/TR01, Royal Belgian Institute of Natural Sciences, Operational Directorate Natural Enviroment, Brussels, 47 pp.

Van den Eynde D. 2016. The impact of extraction on the bottom shear stress in Zone 4. Report ZAGRI-MOZ4-INDI67/1/DVDE/ 201604/EN/TR01, Royal Belgian Institute of Natural Sciences, Operational Directorate Natural Enviroment, Brussels, 52 pp.

Van den Eynde D. 2017. The impact of extraction on the bottom shear stress using the proposed new extraction limit levels. Report ZAGRI-MOZ4-IND67/1/DVDE/201706/EN/TR02, 37 pp.

Van den Eynde D, Francken F, Van Lancker V. 2017. Effects of extraction of sand on the bottom shear stress on the Belgian Continental Shelf. Proc. Studiedag Zand en Grind – Belgisch zeezand – een schaars goed? 9 June, Ostend (Belgium), 20pp.

Van Lancker V, Francken F, Kint L, Montereale-Gavazzi G, Terseleer N, Van den Eynde D. 2016. Large dunes hosting hotspots of biodiversity: Testing proxies of occurrence and habitat change. In: Van Landeghem K, Garlan T, Baas J (Eds.) Proceedings Marine and River Dune Dynamics (MARIDV), 189-192.

Van Lancker V, Baeye M, Evagelinos D, Francken F, Montereale-Gavazzi G, Van den Eynde D. 2017. MSFD-compliant assessment of the physical effects of marine aggregate extraction in the Hinder Banks, synthesis of the first 5 years. Proc. Studiedag Zand en Grind – Belgisch zeezand – een schaars goed? 9 June, Ostend (Belgium), 18pp.

Van Lancker V, Kint L, Montereale Gavazzi G. 2018. Fysische verstoring en verlies van de zeebodem (D6). In: Belgische Staat. Evaluatie van de goede milieutoestand van de Belgische mariene wateren. Kaderrichtlijn Mariene Strategie. BMM, Federale Overheidsdienst Volksgezondheid, Veiligheid van de Voedselketen en Leefmilieu, Brussel, België.

## 7. REFERENCES


Agrawal YC, Pottsmith HC. 2000. Instruments for particle size and settling velocity observations in sediment transport. Marine Geology 168, 89-114.

Agrawal YC, Whitmire A, Mikkelsen Ole A, Pottsmith HC. 2008. Light scattering by random shaped particles and consequences on measuring suspended sediments by laser diffraction. Journal of Geophysical Research 113.

Ainslie MA, McColm JG. 1998. A simplified formula for viscous and chemical absorption in sea water. Journal of the Acoustical Society of America 103, 1671–1672.

Alevizos E, Greinert J. 2018. The hyper-angular cube concept for improving the spatial and acoustic resolution of MBES backscatter angular response analysis. Geosciences 8, 446.

Allen RM, Simeonov J, Calantoni J, Stacey MT, Variano, EA. 2016. Bottom Boundary Layer Turbulence in the California Inner Shelf. 18th PECS Conference, Scheveningen, The Netherlands, Poster.

Andrews S, Nover D, Schladow S. 2010. Using laser diffraction data to obtain accurate particle size distributions: The role of particle composition. Limnology and Oceanogrophy Methods 8, 507–526.

Baeye M, Fettweis M. 2015. In situ observations of suspended particulate matter plumes at an offshore wind farm. Geo-Marine Letters 35, 247-255.

Barter PJ, Deas T. 2003. Comparison of portable nephelometric turbidimeters on natural waters and effluents. New Zealand Journal of Marine and Freshwater Research 37, 485–492.

Becker M, Schrottke K, Bartholom A, Ernstsen V, Winter C, Hebbeln D. 2013. Formation and entrainment of fluid mud layers in troughs of subtidal dunes in an estuarine turbidity zone. Journal of Geophysical Research 118, 2175–2187.

Belgian State. 2012. Determination of good environmental status and establishment of environmental targets for the Belgian marine waters. Marine Strategy Framework Directive – Art 9 & 10. Federal Public Service Health Food Chain Safety and Environment, Brussels, Belgium, 30 pp.

Belgiu M, Drăguţ L. 2016. Random forest in remote sensing: A review of applications and future directions. ISPRS Journal of Photogrammetry and Remote Sensing 114, 24–31.

Bi Q, Toorman EA. 2015. Mixed-sediment transport modelling in the Scheldt estuary with a physics based bottom friction law. *Ocean Dynamics* 65, 555-587.

Blott, S.J., Pye, K., 2001. GRADISTAT: a grain size distribution and statistics package for the analysis of unconsolidated sediments. Earth Surface Processes and Landforms 26, 1237–1248.

Braimoh AK. 2006. Random and systematic land-cover transitions in northern Ghana. Agriculture, Ecosystems & Environment 113, 254–263.

Breiman L. 2001. Random forests. Machine Learning 45, 5–32.

Bright CE, Mager SM, Horton SL. 2018. Predicting suspended sediment concentration from nephelometric turbidity in organic-rich waters. River Research and Applications 34, 629-639.

Buhl-Mortensen L, Galparsoro I, Vega Fernández T, Johnson K, D'Anna G, Badalamenti F, Garofalo G, Carlström J, Piwowarczyk J, Rabaut M, Vanaverbeke J, Schipper C, van Dalfsen J, Vassilopoulou V, Issaris Y, van Hoof L, Pecceu E, Hostens K, Pace ML, Knittweis L, Stelzenmüller V, Todorova V, Doncheva V. 2017. Maritime ecosystem-based management in practice: Lessons learned from the application of a generic spatial planning framework in Europe. Marine Policy 75, 174-186.

Burgass MJ, Halpern BS, Nicholson E, Milner-Gulland EJ. 2017. Navigating uncertainty in environmental composite indicators. Ecological Indicators 75, 268-278.

Capuzzo E, Stephens D, Silva T, Barry J, Forster RM. 2015. Decrease in water clarity of the southern and central North Sea during the 20th century. Global Change Biology 21, 2206–2214.

Cellino M. 1998. Experimental study of suspension flow in open-channels. PhD thesis, Dept. de Génie Civil, Ecole Polytechnique Fédérale de Lausanne.

Chapalain M. 2019. Dynamique des matières en suspension en mer côtière : caractérisation, quantification et interactions sédiments/matière organique. PhD thesis. Université de Bretagne occidentale, Brest (France). 292pp + app.

Chapalain M, Verney R, Fettweis M, Jacquet M, Le Berre D, Le Hir P. 2019. Investigating suspended particulate matter in coastal waters using fractal theory. Ocean Dynamics, 69, 59-81.

Chen S, Eisma D. 1995. Fractal geometry of in situ flocs in the estuarine and coastal environments. Netherlands Journal of Sea Research 33, 173–182.

Congalton RG. 1991. A review of assessing the accuracy of classifications of remotely sensed data. Remote Sensing of Environment 37, 35–46.

Crowder L, Norse E. 2008. Essential ecological insights for marine ecosystem-based management and marine spatial planning. Marine Policy 32, 772-778.

Dale VH, Beyeler SC. 2001 Challenges in the development and use of ecological indicator; Ecological Indicator 1, 3-10.

Davies EJ, Nimmo-Smith WAM, Agrawal YC, Souza AJ. 2012. LISST-100 response to large particles. Marine Geology 307-310.

De Mesel I, Van Lancker V, Kapasakali D, Montereale Gavazzi G, Kerckhof F, Van Hoey G, Wittoeck J, Hillewaert H, Ranson J, Vanelslander B, Hostens K. 2017. Analyse van de huidige status van de bodemfauna in de bodembeschermingszones in de Vlaamse Banken. Federale Overheidsdienst Volksgezondheid, Veiligheid Van De Voedselketen En Leefmilieu, Directoraat-Generaal Leefmilieu, Dienst Marien Milieu, met als projectnummer DG5/MM/SVG/16013.

Desmit X, Thieu V, Billen G, Campuzano F, Dulière V, Garnier J, Lassaletta L, Ménesguen A, Neves R, Pinto L, Silvestre M, Sobrinho JL, Lacroix G. 2018. Reducing marine eutrophication may require a paradigmatic change. Science of the Total Environment 635, 1444-1466.

Diesing M, Green SL, Stephens D, Lark RM, Stewart HA, Dove D. 2014. Mapping seabed sediments: comparison of manual, geostatistical, object-based image analysis and machine learning approaches. Continental Shelf Research 84, 107–119.

Diesing M, Stephens D. 2015. A multi-model ensemble approach to seabed mapping. Journal of Sea Research 100, 62–69.

Downing A, Thorne PD, Vincent CE. 1994. Backscattering from a suspension in the near field of a piston transducer. Journal of the Acoustical Society of America 97 (3), 1614–1620.

Downing J. 2005. Turbidity Monitoring. In: Down RD, Lehr JH (Eds.), Environmental Instrumentation and Analysis Handbook, John Wiley & Sons Inc.

Downing J. 2006. Twenty-five years with OBS sensors: the good, the bad, and the ugly. Continental Shelf Research 26, 2299–2318.

Drake DE, Cacchione DA, Grant WD. 1992. Shear stress and bed roughness estimates for combined wave and current flows over a rippled bed. Journal of Geophysical Research 97, 2319-2326.

Droppo IG. 2001. Rethinking what constitutes suspended sediment. Hydrological Processes 15, 1551-1564.

Droppo I, Leppard G, Liss S, Milligan T. 2005. Flocculation in natural and engineered environmental systems. CRC Press, Boca Raton, Fla, pp. 438.

Druine F, Verney R, Deloffre J, Lemoine J-P, Chapalain M, Landemaine V, Lafite R. 2018. In situ high frequency long term measurements of suspended sediment concentration in turbid estuarine system (Seine Estuary, France): Optical turbidity sensors response to suspended sediment characteristics. Marine Geology 400, 24-37.

Dujardin A, Van den Eynde D, Vanlede J, Ozer J, Delgado R, Mostaert F. 2010. BOREAS - Belgian Ocean Energy Assessment: A comparison of numerical tidal models of the Belgian part of the North Sea. Version 2_0. WL Rapporten, 814_03. Flanders Hydraulics Research, Soresma & MUMM: Antwerp, Belgium. BELSPO contract SD/NS/13A, 62 pp.

Dyer KR, Soulsby RL. 1988. Sand transport on the continental shelf. Annual Review of Fluid Mechanics, 20, 295-324.

Dyer KR. 1989. Sediment processes in estuaries: Future research requirements. Journal of Geophysical Research 94, 14327-14339.

Dyer KR, Manning AJ. 1999. Observation of the size, settling velocity and effective density of flocs, and their fractal dimensions. Journal of Sea Research 41, 87–95.

Dyer KR, Christie MC, Manning AJ. 2004. The effects of suspended sediment on turbulence within an estuarine turbidity maximum. Estuarine, Coastal and Shelf Science, 59, 237-248.

EC-MSFD. 2008. Directive of the European Parliament and the Council Establishing a Framework for Community Action in the Field of Marine Environmental Policy (Marine Strategy Framework Directive), European Commission, Directive 2008, 2008/56/ EC, OJ L, 164pp.

Eigaard OR, Bastardie F, Hintzen NT, Buhl-Mortensen L, Buhl-Mortensen P, Catarino R, Dinesen GE, Egekvist J, Fock HO, Geitner K, Gerritsen HD, Marín González M, Jonsson P, Kavadas S, Laffargue P, Lundy M, Gonzalez-Mirelis G, Nielsen JR, Papadopoulou N, Posen PE, Pulcinella J, Russo T, Sala A, Silva C, Smith CJ, Vanelslander B, Rijnsdorp AD. 2016. The footprint of bottom trawling in European waters: distribution, intensity and seabed integrity. ICES Journal of Marine Science 74, 847-865.

Eisma D. 1986. Flocculation and de-flocculation of suspended matter in estuaries. Netherlands Journal Sea Research 20, 183–199.

Elgar S, Raubenheimer B, Guza RT. 2005. Quality control of acoustic Doppler velocimeter data in the surfzone. Measurement Science and Technology 16, 1889-1893.

EPA. 1993. Method 180.1 - Determination of turbidity by nephelometry (revision 2.0), Environmental Protection Agency, Cincinnati, 10.

Fall KA, Friedrichs CT, Massey GM, Bowers DG, Smith J. 2018. The importance of organic matter content to fractal particle properties in estuarine surface waters as constrained by floc excess density, floc apparent density, and primary particle bulk density: Insights from video settling, LISST, and pump sampling. AGU Fall Meeting, Washington DC (USA), 10-14 December.

Fettweis M, Francken F, Pison V, Van den Eynde D. 2006. Suspended particulate matter dynamics and aggregate sizes in a high turbidity area. Marine Geology 235, 63-74.

Fettweis M. 2008. Uncertainty of excess density and settling velocity of mud flocs derived from in situ measurements Estuarine Coastal and Shelf Science 78, 426–436.

Fettweis M, Houziaux J-S, Du Four I, Van Lancker V, Baeteman C, Mathys M, Van Den Eynde D, Francken F, Wartel S. 2009. Long-term influence of maritime access works on the distribution of cohesive sediments: analysis of historical and recent data from the Belgian nearshore area (southern North Sea). Geo-Marine Letters 29, 321-330.

Fettweis M, Baeye M, Van der Zande D, Van den Eynde D, Lee BJ. 2014. Seasonality of floc strength in the southern North Sea. Journal of Geophysical Research 119, 1911-1926.

Fettweis M, Baeye M. 2015. Seasonal variation in concentration, size and settling velocity of muddy marine flocs in the benthic boundary layer. Journal of Geophysical Research 120, 5648-5667.

Fettweis M, Lee BJ. 2017. Spatial and seasonal variation of biomineral suspended particulate matter properties in high-turbid nearshore and low-turbid offshore zones. Water 9, 694.

Fettweis M, Riethmüller R, Verney R, Becker M, Backers J, Baeye M, Chapalain M, Claeys S, Claus J, Cox T, Deloffre J, Depreiter D, Druine F, Flöser G, Grünler S, Jourdin F, Lafite R, Nauw J, Nechad B, Röttgers R, Sotollichio A, Vanhaverbeke W, Vereecken H. 2019. Uncertainties associated with in situ long-term observations of suspended particulate matter concentration using optical and acoustic sensors. Progress in Oceanography 178, 102162.

Folk RL. 1954. The Distinction between grain size and mineral composition in sedimentary-rock nomenclature. Journal of Geology 62, 344–359.

Fonseca LE, Calder BR. 2007. Clustering acoustic backscatter in the angular response space. U.S. Hydrographic Conference. https://scholars.unh.edu/ccom/384.

Francken F, Van den Eynde D. 2010. Calculation of current and wave induced turbulence from high frequency ADV measurements. Technical Report 2010/12/1/Turbulence/EN. Royal Belgian Institute of Natural Sciences, Operational Directorate Natural Environment, Brussels, 14 pp.

Francois RE, Garrison GR. 1982a. Sound absorption based on ocean measurements. Part I: Pure water and magnesium sulfate contributions. Journal of the Acoustical Society of America 72, 896–907.

Francois RE, Garrison, G.R., 1982b. Sound absorption based on ocean measurements. Part II: Boric acid contribution and equation for total absorption. Journal of the Acoustical Society of America 72, 1879–1890.

Fugate DC, Friedrichs CT. 2002. Determining concentration and fall velocity of estuarine particle populations using ADV, OBS and LISST. Continental Shelf Research 22, 1867–1886.

Fugate DC, Chant RJ. 2005. Near-bottom shear stresses in a small, highly stratified estuary. Journal of Geophysical Research, 110, C03022.

Galparsoro I, Connor DW, Borja Á, Aish A, Amorim P, Bajjouk T, Chambers C, Coggan R, Dirberg G, Ellwood H, Evans D, Goodin KL, Grehan A, Haldin J, Howell K, Jenkins C, Michez N, Mo G, Buhl-Mortensen P, Pearce B, Populus J, Salomidi M, Sánchez F, Serrano A, Shumchenia E, Tempera F, Vasquez M. 2012. Using EUNIS habitat classification for benthic mapping in European seas: Present concerns and future needs. Marine Pollution Bulletin 64, 2630–2638.

Giardino A, Monbaliu J. 2006. Shear stress effects on sand bank morphodynamics and sand sorting. In: Tubielewicz A. (Ed.), Coastal dynamics, geomorphology and protection. EuroCoast - Littoral 2006, Gdansk University of Technology, Gdansk, 88-96.

Goossens D. 2008. Techniques to measure grain size distributions of loamy sediments: A comparative study of ten instruments for wet analysis, Sedimentology 55, 65–96.

Graham GW, Davies EJ, Nimmo-Smith WAM, Bowers DG, Braithwaite KM. 2012. Interpreting LISST-100X measurements of particles with complex shape using digital in-line holography. Journal of Geophysical Research 117, C05034.

Grant WD, Madsen OS. 1982. Movable bed roughness in unsteady oscillatory flow. Journal of Geophysical Research 87, C1, 469-481.

Gray JR, Gartner JW. 2009. Technological advances in suspended-sediment surrogate monitoring. Water Resources Research 45, W00D29.

Gross TF, Isley AE, Sherwood CR. 1992. Effective roughness changes during storms on the North California Shelf. Continental Shelf Research 14, 1239-1256.

Goring DG, Nikora V.I. 2002. Despiking acoustic Doppler velocimeter data. Journal of Hydraulics Engineering 128, 117-126.

Günther H, Hasselmann S, Janssen PAEM. 1992. Wamodel Cycle 4. DKRZ Technical Report No. 4, Hamburg, October 1992, 102 pp.

Ha HK, Hsu W-Y, Maa JP-Y, Shao YY, Holland CW. 2009. Using ADV backscatter strength for measuring suspended cohesive sediment concentration. Continental Shelf Research 29, 1310–1316.

Ha HK, Maa JP-Y, Park K, Kim YH. 2011. Estimation of high-resolution sediment concentration profiles in bottom boundary layer using pulse-coherent acoustic Doppler current profilers. Marine Geology 279, 199–209.

Hammerstad E. 2000. Backscattering and seabed image reflectivity. Kongsberg Maritime AS Technical Note, Horten, Norway.

Hartigan JA, Wong MA. 1979. Algorithm AS 136: A K-Means Clustering Algorithm. Applied Statistics 28, 100.

Heink U, Kowarik I. 2010. What are indicators? On the definition of indicators in ecology and environmental planning. Ecological Indicators 10, 584–593.

Hewitt JE, Thrush SF, Legendre P, Funnell GA, Ellis J, Morrison M. 2004. Mapping of marine soft-sediment communities: integrated sampling for ecological interpretation. Ecological Applications 14, 1203–1216.

Hoitink AJF, Hoekstra P. 2005. Observations of suspended sediment from ADCP and OBS measurements in a mud-dominated environment. Coastal Engineering 52, 103–118.

Holdaway GP, Thorne PD, Flatt D, Jones SE, Prandle D. 1999. Comparison between ADCP and transmissometer measurements of suspended sediment concentration. Continental Shelf Research 19, 421–441.

Hughes-Clarke JE, Iwanowska KK, Parrott R, Duffy G, Lamplugh M, Griffin J. 2008. Inter-calibrating multi-source, multi-platform backscatter data sets to assist in compiling regional sediment type maps: Bay of Fundy. In: Proceedings of Canadian Hydrographic Conference and National Surveyors Conference.

Huntley DA. 1988. A modified intertial dissipation method for estimating seabed stresses at low Reynolds numbers, with application to wave/current boundary layer measurements. Journal of Physical Oceanography 18, 339-346.

Huthnance JM, Humphery JD, Knight PJ, Chatwin PG, Thomsen L, White M. 2002. Near-bed turbulence measurements, stress estimates and sediment mobility at the continental shelf edge. Progress in Oceanography 52, 171-194.

Ierodiaconou D, Schimel ACG, Kennedy D, Monk J, Gaylard G, Young M, Diesing M, Rattray A. 2018. Combining pixel and object-based image analysis of ultra-high resolution multibeam bathymetry and backscatter for habitat mapping in shallow marine waters. Marine Geophysical Research 39, 271–288.

Inoue T, Glud RN, Stahl H, Hume A. 2011. Comparison of three different methods for assessing in situ friction velocity: A case study from Lock Etive, Scotland. Limnology and Oceanography: Methods 9, 275-287.

ISO. 1999. Water Quality – Determination of turbidity, ISO Method 7027. International Organization for Standardization, Geneva, Switzerland.

Jago CF, Kennaway GM, Novarino G, Jones SE. 2007. Size and settling velocity of suspended flocs during a Phaeocystis bloom in the tidally stirred Irish Sea, NW European shelf. Marine Ecology Progress Series 345, 51-62.

Khelifa A, Hill PS. 2006. Models for effective density and settling velocity of flocs. Journal of Hydraulic Research 44, 390–401.

Kim SC, Friedrichs CT, Maa JPY, Wright LD. 2000. Estimating bottom stress in tidal boundary layer from acoustic Doppler velocimeter data. Journal of Hydraulic Engineering 126, 399-406.

Kranenburg C. 1994. The fractal structure of cohesive sediment aggregates. Estuarine Coastal and Shelf Science 39, 451–460.

Kursa MB, Rudnicki WR. 2010. Feature selection with the Boruta package. Journal of Statistical Software 36, 1–13.

Lai H, Fang H, Huang L, He G, Reible D. 2018. A review on sediment bioflocculation: Dynamics, influencing factors and modelling. Science of the Total Environment 642, 1184-1200.

Lamarche G, Lurton X. 2018. Recommendations for improved and coherent acquisition and processing of backscatter data from seafloor-mapping sonars. Marine Geophysical Research 39, 5–22.

Lecours V, Dolan MF, Micallef A, Lucieer VL. 2016. A review of marine geomorphometry, the quantitative study of the seafloor. Hydrololgy and Earth System Sciences 20, 3207–3244.

Lecouturier M. 2000. Turbulence and macro-turbulence in the bottom boundary layer downstream of large-scale bedforms: implications for sediment transport. PhD Thesis. University of Southampton, School of Ocean and Earth Science, 113 pp.

Lee B, Toorman E, Molz F, Wang J. 2011. A two-class population balance equation yielding bimodal flocculation of marine or estuarine sediments. Water Research 45, 2131-2145.

Lee BJ, Kim J, Hur J, Choi I-H, Toorman E, Fettweis M, Choi J.W. 2019. Seasonal dynamics of organic matter composition and its effects on suspended sediment flocculation in river water. Water Resources Research, 55, 6968-6985.

Le Hir P, Bassoullet P, Jestin H. 2000. Application of the continuous modeling concept to simulate high-concentration suspended sediment in a macrotidal estuary. Proc. Marine Science 3, 229–247.

Letter JV, Mehta AJ. 2011. A heuristic examination of cohesive sediment bed exchange in turbulent flows. Coastal Engineering, 58, 779-789.

Li J, Tran M, Siwabessy J. 2016. Selecting optimal random forest predictive models: a case study on predicting the spatial distribution of seabed hardness. PloS One 11, e0149089.

Lohrman A, Cabrera R, Gelfenbaum G, Haines J. 1995. Direct measurments of Reynolds stresses with an acoustic Doppler velocimeter. In: Proceedings of the IEEE Fifth Working Conference on Current Measurements, 7-9 February 1995, Saint Petersburg, Florida (USA), 205-210.

Lurton X. 2010. An introduction to underwater acoustics, Principles and applications. Springer Verlag Berlin Heidelberg, 680 pp.

Lurton X, Lamarche G (Eds.). 2015. Backscatter measurements by seafloor-mapping techniques. Guidelines and recommendations. GeoHab report, 200 pp.

Luyten P (Ed.). 2014. Coherens – A coupled hydrodynamic-ecological model for regional and shelf seas: user documentation. Version 2.6. Report of the Royal Belgian Institute for Natural Sciences, Brussels, Belgium, 1554 pp.

MacDonald IT, Vincent CE, Thorne PD, Moate B. 2013. Acoustic scattering from a suspension of flocculated sediments. Journal of Geophysical Research 118, 2581–2594.

Madricardo F, Foglini F, Campiani E, Grande V, Catenacci E, Petrizzo A, Kruss A, Toso C, Trincardi F. 2019. Assessing the human footprint on the sea-floor of coastal systems: The case of the Venice Lagoon, Italy. Scientific Reports 9, 6615

Maerz J, Hofmeister R, van der Lee EM, Gräwe U, Riethmüller R, Wirtz KW. 2016. Maximum sinking velocities of suspended particulate matter in a coastal transition zone. Biogeosciences 13, 4863–4876.

Maggi F. 2005. Flocculation dynamics of cohesive sediment. PhD thesis Delft University, 136pp.

Maggi F. 2009. Biological flocculation of suspended particles in nutrient-rich aqueous ecosystems. Journal of Hydrology 376, 116–125.

Maggi F. 2013. The settling velocity of mineral, biomineral, and biological particles and aggregates in water. Journal of Geophysical Research 118, 2118–2132.

Malarkey J, Davies AG. 2012. A simple procedure for calculating the mean and maximum bed stress under wave and current conditions for rough turbulent flow based on Soulsby and Clarke's (2005) method. Computers and Geosciences, 43, 101-107.

Malarkey J, Baas JH, Hope JA, Aspden, Parson DR, Peakall J, Paterson DM, Schindler RJ, Ye L, Lichtman ID, Bass SJ, Davies AG, Manning AJ, Thorne PD. 2015. The pervasive role of biological cohesion in bedform development. Nature Communications 6, 6257.

Manning AJ, Bass SJ, Dyer KR. 2006. Floc properties in the turbidity maximum of a mesotidal estuary during neap and spring tidal conditions. Marine Geology 235, 193–211.

Markussen TN, Andersen TJ. 2013. A simple method for calculating in situ floc settling velocities based on effective density functions. Marine Geology 344, 10–18.

Mathys P, De Rouck J, Fernandez L, Monbaliu J, Van den Eynde D, Delgado R, Dujardin A. 2011. Belgian ocean energy assessment (BOREAS). Final Report, Belgian Science Policy Office, Brussels, 171 pp.

McAnally WH, Friedrichs C, Hamilton D, Hayter E, Shrestha P, Rodriguez H, Sheremet A, Teeter AM. 2007. Management of fluid mud in estuaries, bays, and lakes. I: Present state of understanding on character and behavior. Journal of Hydraulic Engineering 133, 9–22.

McArthur MA, Brooke BP, Przeslawski R, Ryan DA, Lucieer VL, Nichol S, McCallum AW, Mellin C, Cresswell ID, Radke L. 2010. On the use of abiotic surrogates to describe marine benthic biodiversity. Estuarine, Coastal and Shelf Science 88, 21-32.

Medwin H, Clay CS. 1998. Fundamentals of acoustical oceanography. Academic Press, New York, pp. 712.

Mehta AJ. 1991. Understanding fluid mud in a dynamic environment, Geo Marine Letters 11, 113–118.

Mengual B, Cayocca F, Le Hir P, Draye R, Laffargue P, Vincent B, Garlan T. 2016. Influence of bottom trawling on sediment resuspension in the 'Grande-Vasière' area (Bay of Biscay, France). Ocean Dynamics 66, 1181-1207.

Mengual B, Le Hir P, Cayocca F, Garlan T. 2019. Bottom trawling contribution to the spatio-temporal variability of sediment fluxes on the continental shelf of the Bay of Biscay (France). Marine Geology 414, 77-91.

Merckelbach L.M. 2006. A model for high-frequency acoustic Doppler current profiler backscatter from suspended sediment in strong currents. Continental Shelf Research 26, 1316–1335.

Merckelbach LM, Ridderinkhof H. 2006. Estimating suspended sediment concentration using backscatterance from an acoustic Doppler profiling current meter at a site with strong tidal currents. Ocean Dynamics 56, 153–168.

Mietta F, Chassagne C, Manning AJ, Winterwerp JC. 2009. Influence of shear rate, organic matter content, pH and salinity on mud flocculation. Ocean Dynamics 59, 751-763.

Mikkelsen OA, Hill PS, Milligan TG, Chant RJ. 2005. In situ particle size distributions and volume concentrations from a LISST-100 laser particle sizer and a digital floc camera. Continental Shelf Research 25, 1959–1978.

Mikkelsen O, Hill P, Milligan T. 2006. Single-grain, microfloc and macrofloc volume variations observed with a LISST-100 and a digital floc camera. Journal of Sea Research 55, 87–102.

Mikkelsen OA, Milligan TG, Hill PS, Chant RJ, Jago CF, Jones SE, Krivtsov V, Mitchelson-Jacob G. 2008. The influence of schlieren on in situ optical measurements used for particle characterization. Limnology and Oceanography: Methods 6, 133-143.

Misiuk B, Lecours V, Bell T. 2018. A multiscale approach to mapping seabed sediments. PloS One 13, e0193647.

Montereale-Gavazzi G, Roche M, Lurton X, Degrendele K, Terseleer N, Van Lancker V. 2018. Seafloor change detection using multibeam echosounder backscatter: case study on the Belgian part of the North Sea. Marine Geophysical Research 39, 229–247.

Montereale-Gavazzi G, Roche M, Degrendele K, Lurton X, Terseleer N, Baeye M, Francken F, Van Lancker V. 2019. Insights into the short-term tidal variability of multibeam backscatter from field experiments on different seafloor types. Geosciences 9, 34.

Montereale Gavazzi GOA. 2019. Development of seafloor mapping strategies supporting integrated marine management: application of backscatter by multibeam echosounders. PhD thesis Univ. Ghent, 392pp

Moody JA, Butman B, Bothner MH. 1987. Near-bottom suspended matter concentration on the continental shelf during storms: estimates based on in-situ observations of light transmission and a particle size dependent transmissometer calibration. Continental Shelf Research 7, 609–628.

Muste M, Kim D, Burkhardt A, Brownson Z. 2006. Near-transducer errors in Acoustic Doppler Current Profiler measurements. World Environmental and Water Resources Congress, Omaha (Nebraska, USA), May 21–25.

Nauw JJ, Merckelbach LM, Ridderinkhof H, van Aken HM. 2014. Long-term ferry-based observations of the suspended sediment fluxes through the Marsdiep inlet using acoustic Doppler current profilers. Journal of Sea Research 87, 17–29.

Nechad B, Ruddick K, Neukermans G. 2009. Calibration and validation of a generic multisensor algorithm for mapping of turbidity in coastal waters. In: Proceedings SPIE "Remote Sensing of the Ocean, Sea Ice, and Large Water Regions", SPIE Vol. 7473, 74730H.

Neukermans G, Ruddick K, Loisel H, Roose P. 2012. Optimization and quality control of suspended particulate matter concentration measurement using turbidity measurements. Limnology and Oceanography: Methods 10, 1011–1023.

Nezu I, Nakagawa H. 1993. Turbulence in open-channel flows. IAHR Monograph, A.A. Balkema (Rotterdam, NL), 281pp.

Nystrom EA, Rehmann CR, Oberg KA. 2007. Evaluation of mean velocity and turbulence measurements with ADCPs. Journal of Hydraulic Engineering 133, 1310-1318.

Orpin AR, Ridd PV, Thomas S, Anthony KRN, Marshall P., Oliver J. 2004. Natural turbidity variability and weather forecasts in risk management of anthropogenic sediment discharge near sensitive environments. Marine Pollution Bulletin 49, 602–612.

Ouda M, Toorman EA. 2019. Development of a new multiphase sediment transport model for free surface flows. International Journal of Multiphase Flow 117, 81-102.

OSPAR. 2010. Quality Status Report 2010. OSPAR Commission. London. 176 pp

Pontius RG, Shusas E, McEachern M. 2004. Detecting important categorical land changes while accounting for persistence. Agriculture, Ecosystems & Environment 101, 251–268.

Porskamp P, Rattray A, Young M, Ierodiaconou D. 2018. Multiscale and hierarchical classification for benthic habitat mapping. Geosciences 8, 119.

Rai AK, Kumar A. 2015. Continuous measurement of suspended sediment concentration: technological advancement and future outlook. Measurements 76, 209–227.

Rattray A, Ierodiaconou D, Monk J, Versace V, Laurenson L. 2013. Detecting patterns of change in benthic habitats by acoustic remote sensing. Marine Ecology Progress Series 477, 1–13.

Regnier P, Friedlingstein P, Ciais P, Mackenzie FT, Gruber N, Janssens IA, Laruelle GG, Lauerwald R, Luyssaert S, Andersson AJ, Arndt S, Arnosti C, Borges AV, Dale AW, Gallego-Sala A, Goddéris Y, Goossens N, Hartmann J, Heinze C, Ilyina T, Joos F, LaRowe DE, Leifeld J, Meysman FJR, Munhoven G, Raymond PA, Spahni R, Suntharalingam P, Thullner M. 2013. Anthropogenic perturbation of the carbon fluxes from land to ocean. Nature Geosciences 6, 597–607.

Rice J, Arvanitidis C, Borja A, Frid C, Hiddink JG, Krause J, Lorance P, Ragnarsson SÁ, Sköld M, Trabucco B, Enserink L, Norkko A. 2012. Indicators for sea-floor integrity under the European Marine Strategy Framework Directive. Ecological Indicator 12, 174–184.

Richards SD, Heathershaw AD, Thorne PD. 1996. The effect of suspended particulate matter on sound attenuation in seawater. Journal of the Acoustical Society of America 100, 1447–1450.

Roche M, Degrendele K, Vrignaud C, Loyer S, Le Bas T, Augustin J-M, Lurton X. 2018. Control of the repeatability of high frequency multibeam echosounder backscatter by using natural reference areas. Marine Geophysical Research 39, 89–104.

Röttgers R, Heymann K, Krasemann H. 2014. Suspended matter concentrations in coastal waters: methodological improvements to quantify individual measurement uncertainty. Estuarine, Coastal and Shelf Sciences 151, 148–155

Rymszewicz A, O'Sullivan JJ, Bruen M, Turner JN, Lawler DM, Conroy E, Kelly-Quinn M. 2017. Measurement differences between turbidity instruments, and their implications for suspended sediment concentration and load calculations: a sensor inter-comparison study. Journal of Environmental Management 199, 99–108.

Sadar, M., 1999. Turbidimeter instrument comparison: Low-level sample measurements technical information series. Hach Company, report D90.5, 55pp.

Sahin C, Verney R, Sheremet A, Voulgaris G. 2017. Acoustic backscatter by suspended cohesive sediments: field observations, Seine Estuary, France. Continental Shelf Research 134, 39-51.

Salehi M, Strom K. 2011. Using velocimeter signal to noise ratio as a surrogate measure of suspended mud concentration. Continental Shelf Research 31, 1020–1032.

Schartau M, Riethmüller R, Flöser G, van Beusekom JEE, Krasemann H, Hofmeister R, Wirtz K. 2019. On the separation between inorganic and organic fractions of suspended matter in a marine coastal environment. Progress in Oceanography 171, 231-250.

Schimel ACG, Beaudoin J, Parnum IM, Le Bas T, Schmidt V, Keith G, Ierodiaconou D. 2018. Multibeam sonar backscatter data processing. Marine Geophysical Research 39, 121–137.

Shen X, Lee BJ, Fettweis M, Toorman E. 2018a. A tri-modal flocculation model coupled with TELEMAC for estuarine muds both in the laboratory and in the field. Water Research, 145, 473-486.

Shen X, Toorman EA, Lee BJ, Fettweis M. 2018b. Biophysical flocculation of suspended particulate matters in Belgian coastal zones. Journal of Hydrology, 567, 238-252.

Shen X, Toorman EA, Fettweis M, Lee BJ, He Q. 2019a. Simulating multimodal floc size distributions of suspended cohesive sediments with lognormal subordinates: Comparison with mixing jar and settling column experiments. Coastal Engineering, 148, 36-48.

Shen X, Toorman EA, Lee BJ, Fettweis M. 2019b. Effects of aquatic biofilms on flocculation processes of cohesive sediments: A modeling approach. Journal of Geophysical Research, 124, 4098-4116.

Sheng J, Hay AE., 1988. An examination of the spherical scatterer approximation in aqueous suspensions of sand. Journal of the Acoustical Society of America 83, 598–610.

Sherwood C, Lacy J, Voulgaris G. 2006. Shear velocity estimates on the inner shelf off Grays Harbor, Washington, USA. Continental Shelf Research, 26, 1995-2018.

Smith SJ, Friedrichs CT. 2011. Size and settling velocities of cohesive flocs and suspended sediment aggregates in a trailing suction hopper dredge plume. Continental Shelf Research 31, S50–S63

Snellen M, Gaida TC, Koop L, Alevizos E, Simons DG. 2018. Performance of multibeam echosounder backscatter-based classification for monitoring sediment distributions using multitemporal large-scale ocean data sets. IEEE Journal of Ocean Engineering 1–14.

Soulsby RL. 1995. Bed shear-stresses due to combined waves and currents. In: Advances in Coastal Morphodynamics. Stive MJF, de Vriend HJ, Fredsøe J, Hamm L, Soulsby RL, Teisson C, Winterwerp JC (eds.), 4-20 - 4-23. Delft Hydraulics, The Netherlands.

Soulsby RL. 1997. Dynamics of marine sands. A manual for practical applications. Telford, London, 249 pp.

Soulsby RL, Humphery JD. 1990. Field observations of wave-current interaction at the sea bed. Water Wave Kinematics 178, 413-428.

Soulsby RL, Clarke S. 2005. Bed shear-stresses under combined waves and currents on smooth and rough beds. Report TR 137. HR Wallingford, United Kingdom, 42 pp.

Soulsby RL, Whitehouse RJS. 2005. Prediction of ripple properties in shelf seas. Mark 2 predictor for time evolution. Final technical report prepared for US Office of Naval Research, Contract No. N00014-04-C-0408. Report TR154, HR Wallingford, United Kingdom, 41 pp + App.

SonarScope-Ifremer. http://flotte.ifremer.fr/fleet/Presentation-of-the-fleet/On-board-software/SonarScope.

Spinrad RW, Yentsch CM, Brown J, Dortch Q, Haugen E, Revelante N, Shapiro L. 1989. The response of beam attenuation to heterotrophic growth in a natural population of plankton. Limnology and Oceanography 34, 1601–1605.

Stacey MT, Monismith SG, Burau JR. 1999. Measurements of Reynolds stress profiles in unstratified tidal flow. Journal of Geophysical Research, 104, 10993-10949.

Stanton TK. 1989. Simple approximate formulas for backscattering of sound by spherical and elongated objects. Journal of the Acoustical Society of America 86, 1499–1510.

Stapleton KR, Huntley DA. 1995. Seabed stress determinations using the inertial dissipation method and the turbulent kinetic energy method. Earth Surface Processes and Landforms 20, 807-815.

Stehman SV, Czaplewski RL. 1998. Design and analysis for thematic map accuracy assessment: fundamental principles. Remote Sensing of Environment 64, 331–344.

Stockmann K, Riethmüller R, Heineke M, Gayer G. 2009. On the morphological long-term development of dumped material in a low-energetic environment close to the German Baltic coast. Journal of Marine System 75, 409–420.

Styles R. 2006. Laboratory evaluation of the LISST in a stratified fluid. Marine Geology 225, 151–162.

Tan XL, Zhang GP., Yi H, Reed AH, Furukawa Y. 2012. Characterization of particle size and settling velocity of cohesive sediments affected by a neutral exopolymer. International Journal of Sediment Research 27, 473-485.

Tang FHM, Maggi F. 2016. A mesocosm experiment of suspended particulate matter dynamics in nutrient- and biomass-affected waters. Water Research 89, 76-86.

Thompson C, Amos C, Jones T, Chaplin J. 2003. The manifestation of fluid-transmitted bed shear stress in a smooth annular flume – a comparison of methods. Journal of Coastal Research, 19, 1094-1103.

Thorne PD, Hardcastle PJ, Holdaway GP, Born AJ. 1994. Analysis of results obtained from a triple frequency acoustic backscatter system for measuring suspended sediments. In: Proceedings of the 6th International Conference on Electronic Engineering in Oceanography, vol. 394, pp. 83–89.

Thorne PD, Hanes DM. 2002. A review of acoustic measurement of small-scale sediment processes. Continental shelf Research 22, 603–632.

Thorne PD, MacDonald IT, Vincent CE. 2014. Modelling acoustic scattering by suspended flocculating sediments. Continental shelf Research 88, 81–91.

Thrush SF, Dayton PK. 2002. Disturbance to marine benthic habitats by trawling and dredging: Implications for marine biodiversity. Annual Review of Ecology and Systematics 33, 449–473.

Toorman EA. 2002. Modelling of turbulent flow with suspended cohesive sediment. In: Fine Sediment Dynamics in the Marine Environment (Eds. Winterwerp JC, Kranenburg C). Elsevier Science BV, 155-169.

Trowbridge JH. 1998. On a technique for measurement of turbulent shear stress in the presence of surface waves. Journal of Atmospheric and Oceanic Technology 15, 290–298.

Trowbridge J, Elgar S. 2001. Turbulence measurements in the surf zone. Journal of Physical Oceanography 31, 2403-2417.

Turner JA, Babcock RC, Hovey R, Kendrick GA. 2018. Can single classifiers be as useful as model ensembles to produce benthic seabed substratum maps? Estuarine Coastal & Shelf Science 204, 149–163.

Urick RJ. 1948. The absorption of sound in suspensions of irregular particles. Journal of the Acoustical Society of America 20, 283–289.

Van den Eynde D, Ozer J. 1993. Sediment-Trend-Analyse: Berekening van sedimenttransport met behulp van een mathematisch model. Studie uitgevoerd in opdracht van HAECON NV, betreffende de 'Sediment-Trend-Analyse' (STA) Activiteit 1. Beheerseenheid Mathematisch Model Noordzee, Brussel, 111 pp.

Van den Eynde D. 2013. Comparison of the results of the operational HYPAS and WAM models. Report OPTOS/1/DVDE/201303/EN/TR1, Royal Belgian Institute for Natural Sciences, Operational Directorate Natural Environment, Brussels, Belgium, 39 pp.

Van den Eynde D, Baeye M, Van Lancker V. 2014. Validation of the OPTOS-FIN model in the exploration 4 zone. Report ZAGRI-MOZ4/X/DVDE/201401/EN/TR1, Royal Belgian Institute of Natural Sciences, Operational Directorate Natural Environment, 40 pp.

van Der Veer HW, Bergman MJN, Beukema JJ. 1985. Dredging activities in the Dutch Wadden Sea: Effects on microbenthic infauna. Netherlands Journal of Sea Research 19, 183–190.

van de Velde S, Van Lancker V, Hidalgo-Martinez S, Berelson WM, Meysman FJR, 2018. Anthropogenic disturbance keeps the coastal seafloor biogeochemistry in a transient state; Scientific Reports 8, 5582.

Van Hoey G, Vincx M, Degraer S. 2005. Small- to large-scale geographical patterns within the macrobenthic Abra alba community. Estuarine, Coastal and Shelf Science 64, 751-763.

Van Lancker V, Deleu S, Bellec V, Le Bot S, Verfaillie E, Fettweis M, Van den Eynde D, Pison V, Wartel S, Monbaliu J, Portilla J, Lanckneus J, Moerkerke G, Degraer S. 2004. Management, research and budgetting of aggregates in shelf seas related to end-users (Marebasse). Scientific Report Year 2. Belgian Science Policy Office, 144 pp.

Van Lancker V, Kint L, Montereale-Gavazzi G. 2018. Fysische verstoring en verlies van de zeebodem (D6). In: Belgische Staat. Art. 17 Beoordeling voor de Belgische mariene wateren – Richtlijn 2008/59/EG. Kaderrichtlijn Mariene Strategie. BMM, Federale Overheidsdienst Volksgezondheid, Veiligheid van de Voedselketen en Leefmilieu, Brussel, België. https://odnature.naturalsciences.be/msfd/nl/assessments/2018/page-d6

Vereecke EE. 2019. Simulation of shallow overland flow with a physics-based bottom friction law for rain-induced soil erosion modelling. MSc thesis, Dept. of Civil Engineering, KU Leuven, 122 pp.

Verney R, Deloffre J, Brun-Cottan J-C, Lafite R. 2007. The effect of wave-induced turbulence on intertidal mudflats: Impact of boat traffic and wind. Continental Shelf Research 27, 594–612.

Verney R. 2008. Hydrodynamics and wave parameters calculated from pressure and velocity measurements. Technical Report, Ifremer, Centre of Brest, France, 19 pp.

Verney R, Lafute R, Brun-Cottan J-C. 2009. Flocculation potential of estuarine particles: The importance of environmental factors and of the spatial and seasonal variability of suspended particulate matter. Estuaries and Coasts 32, 678-693.

Voulgaris G, Meyer ST. 2004. Temporal variability of hydrodynamics, sediment concentration and sediment settling velocity in a tidal creek. Continental Shelf Research 24, 1659–1683.

Walter R K, Squibb ME, Woodson CB, Koseff JR, Monismith SG. 2014. Stratified turbulence in the nearshore coastal ocean: dynamics and evolution in the presence of internal bores. Journal of Geophysical Research 119.

WAMDI Group. 1988. The WAM Model – A third generation ocean wave prediction model. Journal of Physical Oceanography 18, 1775-1810.

Wilcock PR. 1996. Estimating local bed shear stress from velocity observations. Water Resources Research 32, 3361-3366.

Wilkinson RH. 1984. A method for evaluating statistical errors associated with logarithmic velocity profiles. Geo-Marine Letters 3, 49-52.

Williams JJ, Bell P, Thorne PD. 2003. Field measurements of flow fields and sediment transport above mobile bed forms. Journal of Geophysical Research 108, 3109.

Willsteed E, Gill AB, Birchenough SNR, Jude S. 2017. Assessing the cumulative environmental effects of marine renewable energy developments: Establishing common ground. Science of the Total Environment 577, 19–32.

Winterwerp JC. 1998. A simple model for turbulence induced flocculation of cohesive sediment. Journal of Hydraulic Research 36, 309–326.

Winterwerp JC. 2002. On the flocculation and settling velocity of estuarine mud. Continental Shelf Research 22, 1339–1360.

Winterwerp JC. 2006. Stratification effects by fine suspended sediment at low, medium and very high concentrations, Journal of Geophysical Research 111, C05012.

Yan J, Tang H, Xiao Y, Li K, Tian Z-J. 2011. Experimental study on influence of boundary on location of maximum velocity in open channel flows. Water Science and Engineering 4(2), 185-191.

Zampoukas N, Piha H, Bigagli E, Hoepffner N, Hanke G, Cardoso AC. 2013. Marine monitoring in the European Union: how to fulfil the requirements for the marine strategy framework directive in an efficient and integrated way. Marine Policy 39, 349–351.

Zhang Q. 2020. PhD thesis, Dept. of Civil Engineering, KU Leuven (in preparation).

Ziegler AC. 2003. Breakout session 1 – Definition of optical methods for turbidity and data reporting. In: Gray JR, Glysson GD (Eds.). Proceedings of the Federal Interagency Workshop on Turbidity and Other Sediment Surrogates, U.S. Geological Survey, USGS Circular 1250, 9–13.

## ANNEX 1: PRESENTATIONS AT SCIENTIFIC AND POLICY RELATED MEETINGS OR CONFERENCES

Backers J. 2016. Instrument related problems with optical backscatter sensors. Workshop on 'Best practice in generating long-term and large-scale data sets of suspended particulate matter concentration', 24-25 February, Brussels (Belgium).

Bi X, Toorman E. 2015. On two-phase/mixture modelling of sediment transport and turbulence modulation due to fluid-particle interactions. INTERCOH, 7-11 September, Leuven (Belgium).

Bi Q, Ernst S, Lee B, Toorman, E. 2016. Implementation of Two-class Population Balance Equation Bimodal Flocculation Model in TELEMAC-3D. TELEMAC-MASCARET User Conference. October, Paris (France).

Chapalain M, Verney R, Druine F, Fettweis M, le Hir P. 2016. Dynamics of suspended particulate matter in coastal waters (the Bay of Seine). Particles in Europe, 3-5 October, Budapest (Hungary).

Chapalain M, Verney R, Fettweis M, Claquin P, Jacquet M, Le Berre D, Le Hir P. 2017. Dynamics of suspended particulate matter in coastal waters (Seine Bay). INTERCOH, 13-17 November, Montevideo (Uruguay).

Chapalain M, Verney R, Fettweis M, Le Berre D, Jacquet M, Le Hir P. 2019. Floc dynamics at the interface between estuaries and coastal seas: from the tidal scale to the seasonal scale. INTERCOH, 13-17 October, Istanbul (Turkey).

Dulière V, Lee BJ, Fettweis M. 2016. Including the observed effect of microbiological activities in a flocculation model. ECSA56. 4-7 September, Bremen (Germany).

Fettweis M, Baeye M, Verney R. 2015. Uncertainty of in situ SPM concentration measurements. INTERCOH, 7-11 September, Leuven (Belgium).

Fettweis M. 2016. Long term measurements of SPM concentration in the Belgian nearshore: How to estimate the uncertainty? Workshop Best practice in generating long-term and large-scale data sets of suspended particulate matter concentration, RBINS 24-25 February, Brussels (Belgium).

Fettweis M, Baeye M. 2016. SPM concentration measurements in low and high turbulent conditions. ECSA56. 4-7 September, Bremen (Germany).

Fettweis M, Baeye M. 2016. SPM concentration measurements in low and high turbulent conditions. Particles in Europe, 3-5 October, Budapest (Hungary).

Fettweis M, Baeye M, Bi Q, Chapalain M, De Bisschop J, Dulière V, Legrand S, Lurton X, Luyten P, Montereale Gavazzi G, Roche M, Shen X, Toorman E, Van den Eynde D, Van Lancker V, Verney R, Zhang Q. 2016. Tools to support the monitoring of MSFD descriptors 6 'Sea-floor integrity' and 7 'Hydrographical conditions'. North Sea Open Science Conference, 7-10 November, Ostend (Belgium).

Fettweis M, Riethmüller R, Verney R, Becker M, Backers J, Baeye M, Chapalain M, Claeys S, Claus J, Cox T, Deloffre J, Depreiter D, Druine F, Flöser G, Grünler S, Jourdin F, Lafite R, Nauw J, Nechad B, Röttgers R, Sotollichio A, Vanhaverbeke W, Van Hoestenberghe T, Vereecken H. 2017. On best practice for in situ high-frequency long-term observations of suspended particulate matter concentration using optical and acoustic systems. INTERCOH, 13-17 November, Montevideo (Uruguay).

Fettweis M. 2018. Dynamics of SPM on regional scales: Challenges and research opportunities. Workshop Algae-Silt Interactions, 31 January, Delft (The Netherlands).

Fettweis M. 2018. Long-term and continuous measurements of SPM dynamics in the Belgian nearshore area. Lifewatch Data Analysis workshop, 22-23 February, Ostend (Belgium).

Fettweis M, Riethmüller R, Verney R, Becker M. 2018. Uncertainties associated with long-term observations of suspended particulate matter concentration using optical and acoustic sensors. 50th International Liege Colloquium on Ocean Dynamics, 28 May - 1 June, Liège (Belgium).

Fettweis M. 2018. Long-term observations of SPM characteristics in the Belgian nearshore area using water samples and optical and acoustical sensors. NCK Theme day "Mud dynamics in the Southern North Sea and its interaction with ecological processes", 7 July, Rotterdam (The Netherlands).

Fettweis M, Legrand S, Luyten P, Dulière V, Montereale-Gavazzi, Toorman E, Shen X, Verney R, Chapalain M. 2019. Physical indicators as early warning of marine ecosystem changes, INDI67 project. Final workshop of the Belspo INDI67 project, 19 June, Brussels (Belgium).

Fettweis M, Riethmüller R, Schartau M, Verney R, Lee BJ. 2019. The composition of suspended particulate matter in coastal areas. INTERCOH, 13-17 October, Istanbul (Turkey).

Legrand S, de la Vallée P, Fettweis M, Van den Eynde D. 2019. How to use bed-shear stress in a MSFD assessment. The example of the Belgian offshore windmill's farms. Final workshop of the Belspo INDI67 project, 19 June, Brussels (Belgium).

Montereale-Gavazzi G. 2016. Benthic Habitat Mapping from Coastal Lagoons to the Northern Seas RCMG Seminars, Renard Centre of Marine Geology, 25 February, Gent (Belgium).

Montereale Gavazzi G, Roche M, Degrendele K, Lurton X, Van Lancker V. 2016. Comparison of supervised and unsupervised benthic habitat classifications: Case study from the Belgian shelf. GEOHAB, 2-6 May, Winchester (UK).

Montereale-Gavazzi G, Lurton X, Van Lancker V, Roche M. 2016. Monitoring seafloor integrity and GES using Hydro-acoustic methods. ECSA56. 4-7 September, Bremen (Germany).

Montereale-Gavazzi G., Roche M, Degrendele K, Baeye M, Francken F, De Bisschop J, Van Lancker V. 2016. Can multibeam-derived acoustic backscatter be used to monitor changes in seabed habitats? North Sea Open Science Conference, 7-10 November, Ostend (Belgium).

Montereale-Gavazzi G, De Bisschop J, Roche M, Degrendele K, Baeye M, Francken F, Van Lancker V. 2017. In-situ appraisal of near-bed and water-column particle transport on MBES backscatter. GeoHAB Biological and Geological seabed mapping Conference. 1-5 May, Halifax (Canada).

Montereale Gavazzi G, Roche M, Lurton X, Van Lancker V. 2018. Field experiments investigating short-term variability of multibeam seafloor backscatter. MIM Seabed Mapping Workshop, 27-28 February, Edinburgh (United Kingdom).

Papili S, Jenkins C, Roche M, Wever T, Lopera O, Van Lancker V. 2015. Influence of shells and shell debris on backscatter strength: investigation using modeling, sonar measurements and sampling on the Belgian Continental Shelf. Conference Seabed and Sediment Acoustics: Measurements and Modelling. 7-9 September, Bath (UK).

Riethmüller R, Fettweis M, Verney R. 2016. On best-practice for long-term observations of total suspended particulate matter. ECSA56, 4-7 September, Bremen (Germany).

Riethmüller R, Fettweis M, Verney R. 2016. Best-practice for long-term observations of total suspended particulate matter in coastal marine environments. ICES Annual Science Conference, 19-23 September, Riga (Latvia).

Roche M, Baeye M, De Bisschop J, Degrendele K, De Mol L, Papili S, Lopera O, Van Lancker V. 2015. Backscatter stability and influence of water column conditions: estimation by multibeam echosounder and repeated oceanographic measurements, Belgian part of the North Sea. Conference Seabed and Sediment Acoustics: Measurements and Modelling. 7-9 September, Bath (UK).

Roche M, De Backer A, Van den Eynde D, et al. 2017. How sustainable in the Belgian sand extraction? Monitoring results and perspectives. Studiedag Zand en Grind: Belgisch zeezand – een schaars goed? 9 June, Ostend (Belgium).

Shen X, Toorman E, Fettweis M. 2017. A tri-modal flocculation model coupled with TELEMAC for suspended cohesive sediments in the Belgian coastal zone. INTERCOH, 13-17 November, Montevideo (Uruguay).

Shen X, 2018. A multi-modal population balance equation coupled with TELEMAC for flocculation processes of biomineral aggregates. Workshop Algae-Silt Interactions, 31 January, Delft (The Netherlands).

Shen X, Toorman E, Lee BJ, Fettweis M. 2019. A population balance model for multi-class floc size distributions of cohesive sediments in Belgian coastal zones. EGU General Assembly, 7 – 12 April, Vienna (Austria).

Shen X, Toorman EA, He Q, Fettweis M. 2019. Multi-class floc size distributions of cohesive sediments at station Xuliujing of the Changjiang River Estuary. Intercoh, 13-17 October, Istanbul (Turkey).

Toorman E. 2015. Multiscale numerical modelling of mixed sediments morphodynamics. Mission Impossible? INTERCOH, 7-11 September, Leuven (Belgium).

Toorman E, Ouda M, Bi Q. 2016. Development of a hybrid two-phase/mixture model for concentrated sediment transport in open channel flow. Symposium on Two-pHase modElling for Sediment dynamicS in geophysical flows. 12-14 September, Tokyo (Japan).

Toorman E. 2016. Presentation on the progress of the 3CPBE flocculation model at progress meetings of the JPI Oceans WEATHER-MIC project, August 2016, Dresden (Germany)

Toorman E. 2017. Presentation on the progress of the 3CPBE flocculation model at progress meetings of the JPI Oceans WEATHER-MIC project, February, Stockholm (Sweden).

Toorman E, Ouda M. 2017. Marine turbulence in nearshore and surfzone areas. Marine Turbulence Re3-visited,49th Liege colloquium & 8th Warnemünde Days, 22-26 May, Liège (Belgium), 98.

Toorman E, Bi Q, Shen X, Jahnke A. 2017. Modelling microplastics dispersal: anthropogenic cohesive particles and their fate in coastal waters. INTERCOH, 13-17 November, Montevideo (Uruguay).

Toorman E. 2017. Laminar, intermittent and turbulent fluid mud flow. Cohesive Sediment Transport Processes. INTERCOH. 13-17 November, Montevideo (Uruguay).

Van den Eynde D, Baeye M, Fettweis M, Francken F, Van Lancker V. 2015. Validation of modelled bottom shear stress under the influence of currents and waves using long-term measurements. INTERCOH, 7-11 September, Leuven (Belgium).

Van den Eynde D, Baeye M, Fettweis M, Francken F, Van Lancker V. 2016. Changes in bottom shear stress, due to aggregate extraction, in the area of the Hinder Banks (Belgian Continental Shelf). VLIZ Marine Science Day, 12 February, Brugge.

Van den Eynde D, Baeye M, Fettweis M, Francken F, Van Lancker VRM. 2016. Changes in bottom shear stress, due to aggregate extraction in the area of the Hinder Banks (Belgian Continental Shelf). ICES Annual Science Conference, 19-23 September, Riga (Latvia).

Van den Eynde D, Baeye M, Fettweis M, Francken F, Van Lancker V. 2016. Changes in bottom shear stress, due to aggregate extraction, in the area of the Hinder Banks (Belgian Continental Shelf). 18th PECS Conference. 9-14 October, Scheveningen, The Netherlands.

Van den Eynde D, Baeye M, Fettweis M, Francken F, Van Lancker V. 2016. Effect of aggregate extraction on MSFD descriptor 7 (hydrographic condition) in the Hinder Banks area (Belgian Continental Shelf). North Sea Open Science Conference, 7-10 November, Ostend, Belgium.

Van den Eynde D, Baeye M, Fettweis M, Francken F, Van Lancker V, Terseleer N. 2019. Bottom shear stress as an indicator in the MSFD Framework. Final workshop of the Belspo INDI67 project, 19 June, Brussels (Belgium).

Van Hoey G, Devriese L, Dewitte B, Fettweis M, Lauwaert B, Parmentier K, Vanlede J, Hostens K, Martens C. 2016. Environmental impact assessment in line with the EU Nature Directives. North Sea Open Science Conference, 7-10 November, Ostend (Belgium).

Van Lancker V, van Heteren S. 2015. Biotope mapping in Belgium and the Netherlands. International Workshop on Biotope mapping. 2-3 December, Vilm (Germany).

Van Lancker V. 2016. Potential of hydro-acoustic mapping for biodiversity studies. STopP Symposium ‘From Sediment to Top Predator’. 10 February, Büsum (Germany).

Van Lancker V, Kint L, van Heteren S. 2016. Multi-criteria resource mapping and its relevance in the assessment of habitat changes. Ocean Sciences. 21-26 February, New Orleans (USA).

Van Lancker VRM, Baeye M, Evagelinos D, Montereale Gavazzi G, Terseleer N, Van den Eynde D. 2016. MSFD-compliant investigative monitoring of the effects of intensive aggregate extraction on a far offshore sandbank, Belgian part of the North Sea. ICES Annual Science Conference, 19-23 September, Riga (Latvia).

Van Lancker, VRM, Baeye M, Evagelinos D, Montereale-Gavazzi G, Terseleer N, Van den Eynde D. 2016. MSFD-compliant investigative monitoring of the effects of intensive aggregate extraction on a far offshore sandbank, Belgian part of the North Sea. North Sea Open Science Conference, 7-10 November, Ostend (Belgium).

Van Lancker V, Montereale Gavazzi G, Roche M, Degrendele K, Deleu S, Papili S, Lopera O, Versteeg W. 2017. Towards a Community of Practice in 4D Seabed Mapping in Belgium, SEACoP. MIM Seabed Mapping Workshop, 4-6 April, Dublin (Ireland).

Van Lancker V. 2017. Marine Geology activities at RBINS. Overview of projects. EuroGeoSurveys meeting. 29 September, Rome (Italy).

Verney R, Chapalain M. 2016. Quantifying SPM in estuaries and coastal seas. Workshop on ‘Best practice in generating long-term and large-scale data sets of suspended particulate matter concentration’, 24-25 February, Brussels (Belgium).

Verney R, Gangloff A, Chapalain M, Le Berre D, Jacquet M. 2016. Floc features in estuaries and coastal seas. 5th Particles in Europe, 3-5 October, Budapest (Hungary).

Verney R, Chapalain M, Fettweis M. 2019. How accurate can we measure SPMC? Final workshop of the Belspo INDI67 project, 19 June, Brussels (Belgium).